Electron Spin Resonance of Hydrogen Atoms in CaF_2*†

J. L. HALL‡ AND R. T. SCHUMACHER§
Carnegie Institute of Technology, Pittsburgh, Pennsylvania
(Received April 4, 1962)

We report the results of a detailed investigation of the electron spin resonance of a hydrogen atom in an interstitial position in CaF_2. The following aspects of the problem are treated in detail: (1) apparatus and sample preparation; (2) a spin Hamiltonian with four parameters describing the g value and hfs of the hydrogen atom with the eight equivalent fluorine nuclei surrounding it; (3) the electron-nuclear double resonance (ENDOR) spectrum and the resonance linewidth; and (4) an attempt to calculate the parameters of the spin Hamiltonian starting from atomic and ionic wave functions. Our sample preparation technique has allowed us to deuterate the specimens, and we have obtained spin Hamiltonian parameters for the deuterium center as well. Most of the data were obtained at room temperature, but some data are available on the hydrogen center at 77°K. We have essayed an explanation of the small proton-deuteron and temperature-dependent differences of the spin Hamiltonian parameters.

INTRODUCTION

WE report in this paper the results of a detailed study of the electron spin resonance (ESR) of a hydrogen atom in an interstitial position in fluorite, CaF_2. Because of the well-resolved hyperfine interaction of the unpaired electron with the surrounding nuclei, it has been possible to study the local crystalline environment of the hydrogen atom. In addition to questions of sample preparation and experimental techniques (Sec. I), it will be our object to establish the position of the hydrogen in the lattice and to elucidate the details of its interaction with its environment. We will show that the hydrogen atom is at a body-center position in the simple cubic F^- sublattice of CaF_2. The Ca^{++} ions occupy similar positions, except that they only occupy every other body-center position.

The paramagnetic electron interacts with its proton and the eight surrounding fluorine nuclei. We have been able to fit the resonance spectra with the spin Hamiltonian:

$$\mathcal{H}_s = g\beta S_z H_0 + B\mathbf{I}_p\cdot\mathbf{S} + \sum_{\alpha=1}^{8}\mathbf{S}\cdot\mathfrak{T}^\alpha\cdot\mathbf{I}^\alpha - g_p\beta_N I_z{}^p H_0 - g_F\beta_N\sum_{\alpha=1}^{8} I_z{}^\alpha H_0. \quad (1)$$

The first term is the electronic Zeeman interaction; the second, the electron-proton hyperfine interaction; the third, the electron-fluorine hyperfine interaction (sometimes called superhyperfine interaction), and the last two are the nuclear Zeeman interactions of the proton and the fluorine nuclei, respectively. Each hyperfine tensor $\mathfrak{T}^\alpha$ is axially symmetric and hence reduces to two parameters, $T_{\parallel}{}^\alpha$ and $T_\perp{}^\alpha$. The quantitative description of the spin resonance spectra thus consists of finding the four parameters of this spin Hamiltonian: g, B, $T_{\parallel}$, $T_\perp$. Values of the last three of these may be obtained readily from the approximate eigenvalues of (1). This is done in Sec. II, where the resonance spectra are also displayed and the assignment of the interstitial position to the H atom is justified in detail. Interest in the fourth of these parameters, g, lies principally in its deviation Δg from the value of g for the free hydrogen atom. Δg turns out to be small, and the accurate knowledge of Δg requires knowledge of the positions of the resonance lines to a small fraction of their linewidth. Extraction of Δg from the data thus requires a more accurate knowledge of the eigenvalues of (1) than required to obtain B, $T_{\parallel}$, and $T_\perp$. This is the subject matter of Sec. III. The origin of the linewidth is examined in Sec. IV, where it is shown that the observed widths may be accounted for partly by considerations discussed in Sec. III, but mostly by unresolved hyperfine interactions of the electron with the 24 next-nearest-neighbor fluorine nuclei. These interactions are resolved experimentally by an electron-nuclear double resonance (ENDOR) experiment. Our identification of the center giving rise to the observed resonance spectrum as being atomic hydrogen is strongly supported by our ability to deuterate the samples.

Finally, we believe more than just ordinary interest in this center should arise from attempts to calculate the parameters of the spin Hamiltonian from a wave function of the interstitial atom. The theory of the superhyperfine interactions is related, albeit indirectly, to the theory of superexchange in antiferromagnetic ionic crystals, particularly MnF_2 and $KMnF_3$. The superhyperfine interactions we measure resemble strikingly those in $Mn{:}ZnF_2$, examined experimentally by Tinkham[1] and by Clogston *et al.*,[2] and theoretically by numerous authors.[3] In Sec. V of this report we present

* Supported by a grant from the National Science Foundation.
† Taken in part from a thesis submitted by J. L. Hall in partial fulfillment of the requirements for a Ph.D. degree from Carnegie Institute of Technology.
‡ National Carbon Predoctoral Fellow. Now at National Bureau of Standards, Joint Institute for Laboratory Astrophysics, Boulder, Colorado.
§ Alfred P. Sloan Foundation Fellow.

[1] M. Tinkham, Proc. Roy. Soc. (London) **A236**, 535 (1956).
[2] A. M. Clogston, J. P. Gordon, V. Jaccarino, M. Peters, and L. R. Walker, Phys. Rev. **117**, 1222 (1960).
[3] A comprehensive list of references relating to this and similar problems may be found in the article by W. Marshall and R. Stuart, Phys. Rev. **123**, 2048 (1961).

the results of a simple, standard essay of the calculation of B, T_{II}, and $T_{\perp}$, and a detailed, if inconclusive, study of the temperature dependences and proton-deuteron differences of these parameters.

I. APPARATUS AND EXPERIMENTAL CONSIDERATIONS

A. *X*-Band Spectrometer

Most of the magnetic resonance spectra analyzed in this work have been obtained at room temperature with a high-sensitivity 9 kMc/sec (X band) superheterodyne microwave spectrometer of novel design. In this apparatus we make use of a single klystron superheterodyne, rather than the usual arrangement with a separate local oscillator klystron. This arrangement, to our knowledge, was first suggested by Feher.[4] It not only eliminates the initial expense of duplicate klystron power supply, and frequency stabilization system, but in fact provides a simple way of utilizing the superior sensitivity of a phase-coherent detection system.

A block diagram of the spectrometer is shown in Fig. 1. The necessary local oscillator signal, displaced above (or below) the signal frequency by the i.f. frequency of 63 Mc/sec, is produced by 63-Mc/sec amplitude modulation of a portion of the klystron output power. Use of a balanced modulator bridge, followed by a tuned transmission cavity enables us to obtain sufficient sideband power for optimum operation of the signal circuit mixer crystals (up to 2 mA each), along with adequate suppression of the carrier frequency and the unused sideband. The resonance signal from the balanced signal circuit mixer crystals is fed into a low-noise 63-Mc/sec i.f. amplifier of relatively conventional design. Following about 70 dB of amplification, the resonance signal is coherently detected with a 63-Mc/sec reference signal obtained from the same oscillator which drives the sideband-producing modulator crystals. The phase-detected audio output is finally narrow banded by coherent detection at the magnetic field modulation frequency, and the absorption-derivative lineshape displayed on a dc recorder.

We have found it convenient to lock the klystron frequency to the sample cavity with a frequency-modulation type of automatic frequency control system. Stabilization to the sample cavity, rather than an auxiliary reference cavity as is often done, has the following advantages: (1) It eliminates the need for precise temperature regulation of the two cavities which is otherwise necessary for utilization of the ultimate sensitivity, and (2) the spectrometer responds only to the pure absorption part of the resonance signal, even when the sample bridge is significantly detuned, or when the absorption susceptibility is much smaller than the dispersion susceptibility under strong saturation conditions, for example. These factors both

[4] G. Feher; Bell System Tech. J. 36, 449 (1957).

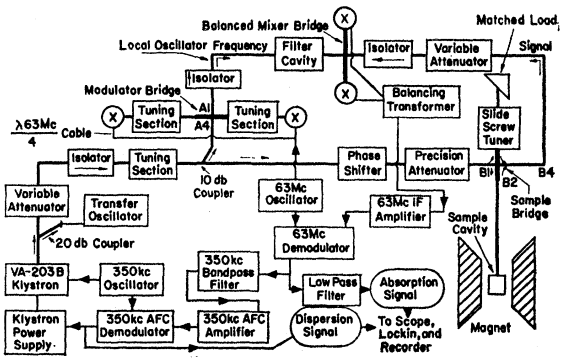

FIG. 1. Block diagram of the coherent superheterodyne X-band paramagnetic resonance spectrometer.

make data easier to obtain and to interpret. The small, for this work, insignificant penalty which must be paid for this convenience is increased noise level of the dispersion signal by a factor of ~5–20 over that of a well-designed separate cavity stabilization scheme.[5]

B. *K*-Band Spectrometer

In order to extract the spin Hamiltonian parameters from the data, large Breit-Rabi corrections (~1%) are required because the external magnetic field is not infinitely large compared with internal magnetic fields. It is therefore of considerable interest to repeat the experiments at a significantly different frequency. We have employed a crystal rectifier frequency doubler to provide output at 18 kMc/sec (K-band) from the 9-kMc/sec input obtained from the existing klystron and microwave layout. By the use of relatively concentrated sample crystals, useful spectra could be obtained with a simple superheterodyne circuit equivalent to the now famous "i.f.-type Pound stabilizer." The frequency doubler crystal is partially amplitude modulated at 63 Mc/sec. By proper adjustment of the reverse biasing network, we can produce an 18-kMc/sec carrier with 63-Mc/sec sidebands by this process. The microwave electric field reaching the K-band mixer crystal thus has three component frequencies, each of which is treated differently by the K-band sample bridge. The carrier frequency, equal to the resonant frequency of the sample cavity, is more or less completely absorbed in the cavity. The reflected wave at this frequency contains the ESR signal. The two sideband frequencies are essentially totally reflected by the cavity and form the "local oscillator" signal at the mixer crystal. By employing an overcoupled sample cavity, the sample bridge imbalance may be decreased at the carrier frequency and increased at the sideband

[5] Since the work described here was completed, the sample bridge system using a magic tee has been replaced by a microwave circulator. The cavity is matched by a minor variant of the variable coupling scheme of J. Gordon [Rev. Sci. Instr. 32, 658 (1961)]. The revised system works at least as well as the older system, and we have no reason to believe we have not increased the signal-to-noise ratio by the factor of two expected by the use of the circulator.

frequencies by the *same* setting of the adjustable reference reflection. Normal superheterodyne operation is obtained because the two 63-Mc/sec beat notes of the resonance signal with the two sideband signals are essentially in phase, and hence can be fed into the 63-Mc/sec amplifier and processed as usual. Even the same AFC system may be used.

Although the microwave power level is relatively unadjustable, the 50 to 100 μW K-band power we obtain is conveniently near, but safely below, the onset of saturation of the H atom resonance lines. At this microwave power level we estimate the sensitivity of this apparatus to be roughly 50× less than the high-sensitivity X-band spectrometer previously described.

C. ENDOR

Our electron-nuclear double resonance (ENDOR) data have been obtained at 77°K with a repetitive form of Feher's "transient, spin-packet-shifting" type of double resonance effect.[6] This natural extension of Feher's method does not appear to have been fully exploited previously, although it offers two very significant advantages.[6a] (1) The signal-to-noise ratio is much larger than the usual "single-shot" signal, by a factor $\sim$(integrating time constant)×(repetition frequency) $\simeq$50× in our case. This allows one to study resonances exhibiting a much lower degree of inhomogenous broadening than the classical F center, for example, or to operate at a much more convenient temperature than the low helium range which is usually required. (2) The line shape of the output signal, under suitable experimental conditions, is directly the nuclear magnetic resonance (NMR) lineshape of the particular class of nuclei being investigated. By contrast, in the "single-shot" technique, the lineshape is essentially determined by experimental parameters such as microwave power level and rate of change of the nuclear probing oscillator's frequency.

The ENDOR technique is of interest in the study of ESR lines which are inhomogeneously broadened by nonresonant interactions, for example by unresolved hyperfine interactions with nearby nuclei. The physical mechanism of repetitive ENDOR is discussed more fully in the following several paragraphs, but it is convenient to begin with a simple operational description. The static magnetic field is first adjusted to satisfy the spin resonance condition and the field modulation switched off. The microwave power is increased to provide moderate saturation of the ESR transition. With an auxiliary radio-frequency magnetic field, nuclear transitions are induced which convert resonant centers into nonresonant ones, and vice versa. By square-wave amplitude modulating the nuclear oscillator, we cause a corresponding periodic disturbance of the populations of the electronic spin states. The resulting ripple on the absorption signal from the spectrometer is narrow banded by synchronous detection at the square-wave frequency, and the rectified dc is stored in an integrating capacitor. This voltage is displayed on a dc recorder and the ENDOR line is scanned by slowly varying the nuclear oscillator frequency.

The choice of frequency for the square-wave modulation is obviously governed by the effective spin-lattice relaxation time. If the modulation frequency is too high, the nonresonant spin systems do not have enough time to recover to the lattice temperature while they are thermally disconnected from the microwave source. If the square-wave frequency is too low, the transient increase in ESR absorption when the nuclear oscillator is switched on will occupy too small a fraction of the modulation period. A reasonable estimate of the optimum modulation period is simply the spin-lattice relaxation time T_1. A similar reasonable choice of microwave power level would make the microwave saturating time approximately one-half T_1. In the present case, T_1 at nitrogen temperature is roughly 10 msec and a pre-existing 38 cps "twin tee" amplifier was advantageously employed. ENDOR signals were about four times smaller at 350 cps than at 38 cps; lower modulation frequencies were not tried.

The effectiveness of this technique clearly depends upon the thermal insulation between the several spin packets that form the observed inhomogeneously broadened ESR line. If the spin packets which are interconverted by the nuclear transitions are separately in thermal contact with the microwave radiation field, obviously no disturbance of the electronic populations is to be expected. We believe that such effects are involved in the rather drastic decrease of ENDOR signal strength of a heavily doped sample ($\sim 10^{19}$H atoms/cm^3) for nuclear probing frequencies within about 100 kc/sec of the fluorine Larmor frequency.

Further support for such a spin diffusion type of explanation derives from ESR experiments employing the saturation curve technique of Castner.[7] In this way, we find at room temperature that the ESR line appears to be composed of about 20 distinct spin packets, each with its own slightly different resonant field, H_0. At nitrogen temperature, however, the apparent spin-lattice relaxation time has increased by about 300× and the slow process which involve energy exchange between spin systems resonant at *almost* the same frequency become relatively more important. Thus the saturation curve technique, which gives the estimate of 20 different types of magnetic environments at room temperature, gives at nitrogen temperature the estimate of 2.5 different types.

Although this treatment is perhaps incomplete in that it ignores Redfield-type saturation behavior,[8] the

[6] G. Feher, Phys. Rev. **114**, 1219 (1959).

[6a] *Note added in proof.* The first complete exploitation of this technique seems, in fact, to have been by H. Seidel, whose work is described in Z. Physik **165**, 218, 239 (1961).

[7] T. G. Castner, Jr., Phys. Rev. **115**, 1506 (1959).

[8] A. G. Redfield, Phys. Rev. **98**, 1787 (1955).

following qualitative conclusion appears still to be valid: The electron T_1 at nitrogen temperature is sufficiently long to allow spin excitation, before ultimately being diverted to the lattice by a T_1 process, to leak into spin packets separated in resonant frequency from the microwave frequency by many packet widths. Operationally this effect results in reduced sensitivity to distant, weakly coupled nuclei.

The microwave cavity used for these double-resonance experiments is essentially the same as the conventional $\frac{1}{2}\lambda g$ cavity used in the ESR experiments, except that it contains a heavy vertical copper wire about 3 mm from the narrow vertical wall.[9] This wire carries several amperes of 12-Mc/sec current, thus producing the 12-Mc/sec magnetic field necessary to induce the desired $\Delta M_{\text{fluorine}} = \pm 1$ transitions. The wire is excited through a low-impedance transmission line ($\sim 0.5\Omega$) from a toroidal impedance matching transformer located well outside the magnet gap. With about 15 W dc input to the untuned class-A buffer amplifier we obtain several gauss over a bandwidth of 10 Mc/sec. By using about 50 W dc input to a class-C oscillator, more than 10 G (rotating) is readily available in the sample.

D. Sample Preparation

Our recipe for production of interstitial hydrogen atoms in CaF_2 is the following:

1. "Pure" CaF_2 crystals, obtained from Harshaw, and aluminum metal are well outgassed just below the melting point of the metal. For the magnetic resonance experiments, using CaF_2 as free as possible from paramagnetic ions is very important in order to avoid spurious resonances. The common impurities in aluminum do not seem to give any difficulties: Perfectly satisfactory samples were prepared even with chips of commercial "2S" aluminum sheet.

2. A few cm of Hg pressure of H_2 (or D_2) is (cautiously) admitted; the temperature is increased to 900°C and maintained for a few hours.

3. After cooling and mechanical removal of excess aluminum, the crystals are lightly acid etched and x rayed for a few hours (typically 4 h at 30 kV and 30 mA). After x raying, the crystals appear very black in reflection and essentially opaque in transmission for crystals as thin as 1 mm.

4. The crystals are cleaved to the desired size. It is useful to start with crystals of sufficient size that all new surfaces may be exposed: this gives sharp edges which aid in aligning the crystal in the microwave cavity and prevents loss of cavity Q if a small amount of metallic aluminum happens to remain on the surface.

5. Results—We have obtained densities of interstitial atomic hydrogen as high as $10^{19}/cm^3$ with this technique. The samples are thermally stable to at least +50°C, but appear to deteriorate slowly in a few months' time. Apparently no other paramagnetic centers are produced.

There are obviously some interesting questions to be asked regarding the formation and stabilization of atomic hydrogen in CaF_2: in the present paper we shall confine our attention to the (at least) equally interesting magnetic properties of the resulting samples.

Since first reporting this work[10] we have received private communications reporting the observations of resonances our communicants believe to be of the same origin as those we report here. Paul Handler, University of Illinois, evidently was able to introduce or "activate" hydrogen atoms in CaF_2 by sustaining a gaseous discharge in tubes containing CaF_2 powder. Jerome Sierro has reported privately to us the observation of similar resonances in natural samples of CaF_2. We have also found that weak resonances may be seen by repeating the treatment described above with the substitution of He gas or a vacuum for the H_2 gas. Evidently both natural and synthetic fluorite contain hydrogen in some form.

II. DETERMINATION OF THE SPIN HAMILTONIAN

All of the magnetic resonance experiments performed on CaF_2 crystals prepared as described are consistent with the model in which an electrically neutral hydrogen atom is located at one of the body centers of the simple cubic sublattice formed by the fluorines of CaF_2. The "box" formed by the eight nearest-neighbor fluorines is sufficiently large and the hydrogen atom sufficiently small that the crystal lattice is probably essentially undilated by the presence of the hydrogen, (see, however, Sec. V) and, in any event the full cubic symmetry is preserved. The hydrogen atom (in its ground state) and the eight fluorine ions interact remarkably weakly, and the hydrogen atom may still be regarded to a very good approximation as existing as an undisturbed atom in its spherically symmetric ground electronic state. It is the spin of this unpaired hydrogen electron which is involved in all the resonance experiments to be described.

The experimental electron spin resonance spectra show the strong hyperfine interaction of the electron with a spin-$\frac{1}{2}$ nucleus (proton) plus a somewhat weaker hyperfine interaction with eight equivalent spin-$\frac{1}{2}$ nuclei (F^{19}). Thus one sees two main groups of resonance lines, corresponding to the two orientations of the proton magnetic moment in the external field. If pure CaF_2 crystal is "doped" with deuterium rather than hydrogen, the ESR pattern consists of 3 main groups of lines separated by a much smaller magnetic field of the centers of the groups, due to hyperfine coupling with the proton or deuteron, is found to be in the same ratio as their magnetic moments. Crystals prepared in an atmosphere of 1/2 hydrogen, 1/2 deu-

[9] This very effective technique was patterned after a much more elegant cavity design by Dr. J. Townsend of Washington University in St. Louis, Missouri.

[10] J. L. Hall and R. T. Schumacher, Bull. Am. Phys. Soc. **6**, 247 (1961).

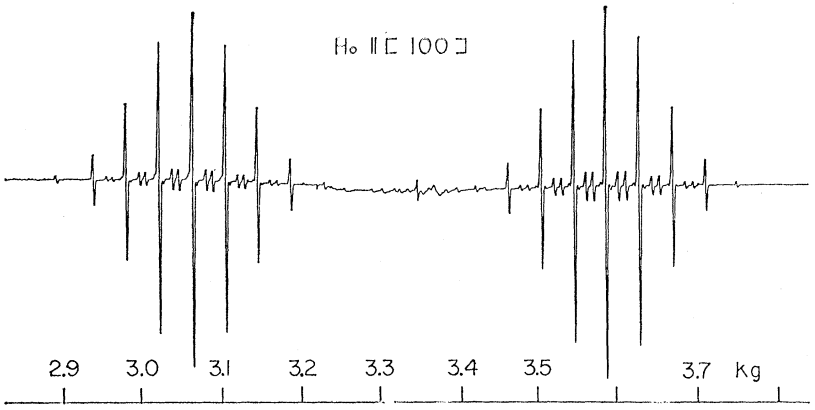

FIG. 2. ESR absorption derivative, $H_0 \| [100]$. The two nine-line patterns correspond to the two proton spin orientations. The prominent doublets between the larger resonance are the forbidden transitions discussed in the text. The sharp line at 3.35 kG is a g marker. The other small resonances near $g=2.00$ are from impurities or are from $\Delta M_s=\pm 1$, $\Delta M=\pm 1$ transitions induced by components of $H_1 \| H_0$.

terium, show both types of resonance patterns with equal total intensity in each; crystals heat-treated in the same manner but in vacuum show no resonances of this type.

In CaF_2, the fluorine system forms a simple cubic lattice with the F^- ions at the corners. The Ca^{++} occupy alternate body centers: Because of the divalency of calcium, only 1/2 as many Ca^{++} ions as F^- ions are needed to establish local charge neutrality. There are accordingly a large number of unoccupied body-center sites at which a neutral atom could be located. Each hydrogen atom then has eight geometrically equivalent nearest-neighbor fluorine ions with a hydrogen-fluorine "center-center" distance $R=\sqrt{3}a/2=2.36$ Å. The fluorine ionic radius of 1.36 Å leaves 1.00 Å for the maximum radius of the hydrogen atom in this hard sphere picture. All but 8% of the charge of an isolated hydrogen atom would be contained within such a 1 Å radius shell. While such an estimate would only be really significant if it were to show that enormous lattice distortion was necessary to accommodate the hydrogen, the result that the model is self-consistent in the hard-sphere approximation is at least comforting. The electron spin resonance data are entirely consistent with the model in all the detailed predictions one may make based upon it, even including the angular variation of the ENDOR resonances of the second and third shell of fluorine ions.

The spin resonance spectrum of the interstitial hydrogen atom with the external magnetic field H_0 aligned parallel to the [100] direction of the CaF_2 crystal is shown in Fig. 2. This resonance spectrum is observed to consist of two main groups of nine lines each. As pointed out above, the large spacing in magnetic field between the centers of the two patterns is due to the hyperfine interaction of the electron and proton. The smaller spacing between the nine lines of each group is caused by the hyperfine interaction with the eight fluorine spins.

One may think in semiclassical terms that the electron has a characteristic magnetic field in which spin resonance occurs, which depends only on the microwave frequency and the (fixed) magnetic moment of the electron. The proton and the various fluorines generate *internal local* magnetic fields which can add to or subtract from the externally applied field. Thus, several different values of external field can give rise to electron spin resonance, corresponding to the several possible values of the internal field. For example, the low-field group of lines corresponds to the proton magnetic moment aligned parallel to the external field; the lowest (weak) line of the low-field group corresponds to all of the eight fluorines, as well as the proton moment, aligned parallel to the external field. The next to lowest line of the low-field group results from seven fluorine moments parallel and one antiparallel. The third line, from 6 parallel, 2 antiparallel, etc. The highest line of the low-field group corresponds to proton parallel and all eight fluorines antiparallel to the external field.

The intensity ratios between the nine lines of each main group establish the magnetic equivalence of the eight F^- ions: The arrangement of fluorine nuclei in which all eight are parallel to the field is obviously singular. The arrangement with 7 parallel, 1 antiparallel, has a relative strength of eight, since any one of the eight fluorines could be the antiparallel one. The arrangement with 6 and 2 (the third line) can be obtained in 28 ways; 5 and 3 (the next-to-center line) in 56 ways. The central line, corresponding to four fluorines parallel and 4 antiparallel, can be obtained in 70 ways. The pattern will be symmetric about this central line.

The same arguments give the same predicted pattern for the high-field group, corresponding to the proton moment antiparallel. This set of predicted intensity ratios, 1:8:28:56:70:56:28:8:1, is confirmed experimentally within an experimental scatter of $\sim 3\%$.

Quite clearly, the reason such a simple spectrum exists is that the local field produced by fluorine nucleus j is exactly the same size as that produced by another fluorine nucleus k. We obtain the total local field by counting the number which aid the external field, and subtracting the number which are in opposition: the field interval unit is the same size for each and factors out of the summation. The spacing between

adjacent lines is therefore seen to be the (common) size of the local field. One says the eight fluorine nuclei are magnetically equivalent for H_0 parallel to [100]. We will observe for later use that the vectors from each of the fluorines to the hydrogen atom are parallel to body diagonals of the cube and each makes the same angle $\sim 55°$ with the external field which is parallel to the cube edge.

The well-resolved doublet structure observed between each pair of the main lines in Fig. 2 arises from transitions in which a fluorine nuclear spin as well as the electronic spin reorient in the external field. These "forbidden" transitions are discussed at the end of this section.

We wish now to consider the case in which H_0 makes some arbitrary angle with the crystalline axes. We will allow the most general bilinear dependence of the electron-fluorine hyperfine energy upon the direction of the external field H_0, namely a tensor interaction of the form

$$\mathcal{H}_{\text{hfs}}=\sum_{\alpha=1}^{8} \mathbf{S}\cdot\mathfrak{T}^{\alpha}\cdot\mathbf{I}^{\alpha}.$$

We insist that the interaction energy must be unchanged by any of the symmetry operations which are allowed by the model. Since the body diagonal of a cube is a threefold rotation axis, the hyperfine tensor must be axially symmetric about this direction. Accordingly, the third principal axis of the hyperfine tensor is the body diagonal itself. The angular part of the expansion of the hyperfine energy expression for an arbitrary direction of the magnetic field, then, can be written in terms of θ, the angle between H_0 and the body diagonal which passes through the fluorine of interest. We thus have the result that the two fluorine nuclei which share a given body diagonal are always magnetically equivalent. Since such a pair of nuclei only has three states which differ in energy, the maximum number of different hyperfine energies is reduced from $2^8=256$ to $3^4=81$.

There are four orientations of the crystal in the external field which have been analyzed in detail in this work: H_0 parallel to [100], [111], [110], and [11$\bar{2}$]. At [100], all four pairs of nuclei made the angle $\theta=55°$, giving nine lines as previously discussed. With [110] parallel to H_0, we have two pairs at the angle $\theta=90°$, two pairs at the angle $\theta=35°$. As might be expected, the [110] spectrum (Fig. 3) shows "beating" as the two characteristic values of hyperfine splitting are combined with various signs and strengths, corresponding to the various different configurations of parallel and antiparallel fluorine nuclei. A maximum number of $5\times5=25$ transitions are expected and 25 are observed. The two characteristic splittings are easily obtained from such data, but at this stage we do not know whether the larger splitting corresponds to $\theta=90°$, or $\theta=35°$.

For H_0 aligned parallel to [111], there are three pairs of fluorine nuclei at $\theta=71°$ and one pair at $\theta=0°$. This spectrum is expected to consist of $7\times3=21$ transitions: each of the seven lines due to the three pairs at 71° is split into 3 by the pair at $\theta=0°$. The experimental spectrum, Fig. 4, is seen to contain 11 principal lines. By the assumption that the splitting due to the 0° group is twice that due to the 71° groups, one can synthesize an 11-line spectrum with the following intensity ratios: 1:6:17:32:46:52:46:32:17:6:1. These intensities are in agreement with the experimental values after the latter are corrected for the small variations in width of the experimental resonance lines, caused by the ratio of the two splittings not being exactly two.

The fourth case which has been analyzed in detail is for H_0 parallel to [11$\bar{2}$]. This produces two pairs of fluorines at $\theta=65°$ and one pair each at 90° and 19°. This spectrum consists of $3\times3\times5=45$ lines, several of which may be expected to be nearly degenerate. By employing the smaller of the two candidates for the 90° hyperfine splitting as determined from the [110] spectrum, the 25 lines of the observed spectrum can be easily unraveled to yield the hyperfine splitting constants at 19°, 65° and to redetermine the 90° splitting.

It is perhaps worth emphasizing that implicit in this qualitative discussion of the spectra has been the assumption that the eight fluorine hyperfine tensors are

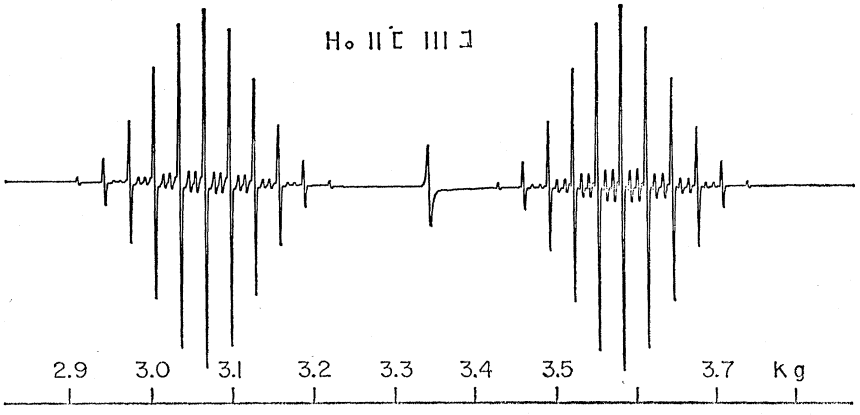

FIG. 3. ESR absorption derivative, $H_0\|[111]$. The origin of the eleven line pattern is discussed in the text. The doublets between the main lines are forbidden transitions, and the line near 3.35 kG is a DPPH g marker. This spectrum was taken with a more concentrated sample than that of Fig. 2.

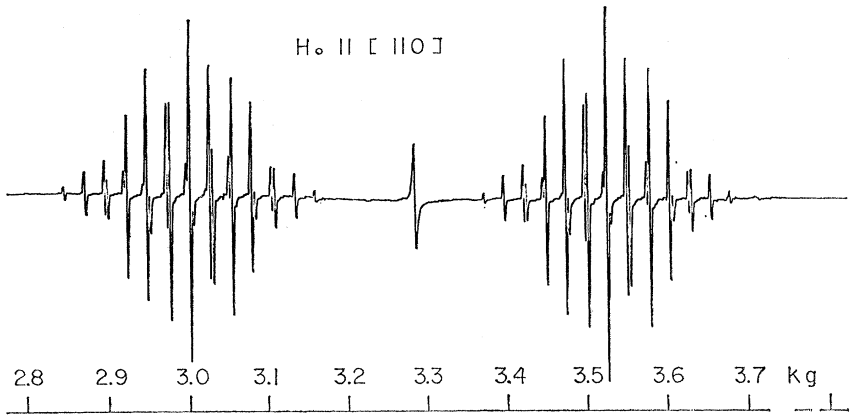

FIG. 4. ESR absorption derivative, $H_0 \| [110]$. Each group consists of 25 lines. The weakest pair in each spectrum is not visible on the figure except for a hint of a line at about 3.71 kG. This spectrum was taken with the same sample and g marker as Fig. 3.

numerically identical, differing only in which of the body diagonals is its symmetry axis. Such equivalence is obviously required by the cubic symmetry of the model. We obtain below a more explicit "quantitative" substantiation of the model from a comparison with experiment of the predicted form of the angular dependence of the hyperfine splitting constant.

For quantitative substantiation of the correctness of our model we must fit the data with the parameters of the spin Hamiltonian

$$\mathcal{H}=g\beta S_z H_0+B\mathbf{I}^p\cdot\mathbf{S}+\sum_{\alpha=1}^{8}\mathbf{S}\cdot\mathfrak{T}^\alpha\cdot\mathbf{I}^\alpha-g_F\beta_N \times\sum_{\alpha=1}^{8}I_z{}^\alpha H_0-g_p\beta_N I_z{}^p H_0. \quad (1)$$

The terms on the right side of (1) are written in order of importance. The first two terms plus the proton Zeeman term form the spin Hamiltonian of the free hydrogen atom. The eigenvalues of this Hamiltonian alone are given by the well-known Breit-Rabi[11] formula:

$$W(F,M_F)=-\tfrac{1}{4}B-g_p\beta_N M_F H_0 \pm[1+2M_F x+x^2]^{1/2}, \quad (2)$$

where

$$x=(g\beta+g_p\beta_N)H_0/B.$$

The plus sign goes with $F=1$, $M_F=\pm1$, 0; the minus sign goes with $F=0$, $M_F=0$. The wave functions which correspond to the indicated energies are:

$$\begin{aligned}
|1\rangle&=|-\rangle|+\rangle-\frac{1}{2x}|+\rangle|-\rangle, && W(0,0)\\
|2\rangle&=|-\rangle|-\rangle, && W(1,-1)\\
|3\rangle&=|+\rangle|-\rangle+\frac{1}{2x}|-\rangle|+\rangle, && W(1,0)\\
4&=|+\rangle|+\rangle. && W(1,1)
\end{aligned} \quad (3)$$

The strong transitions induced by the microwave field obey the rules $\Delta M_s=\pm1$, $\Delta M_p=0$. The "lower field line" thus corresponds to the transition $|1\rangle\leftrightarrow|4\rangle$, the "upper field line" to the transition $|2\rangle\leftrightarrow|3\rangle$.

[11] G. Breit and I. I. Rabi, Phys. Rev. 38, 2082 (1931).

The other two terms of (1) split these upper and lower field lines as discussed qualitatively above. We will treat these terms as a perturbation of the hydrogen atom Hamiltonian whose eigenfunctions and eigenvalues are written above. Although the interaction with the fluorine spin system depends on which of the four eigenstates of the hydrogen atom problem is being considered, we will find it convenient to write the fluorine hyperfine interaction in terms of M_s, taking the state mixture demonstrated in (3) into account later. In this sense the fluorine-electron interaction does not depend on the proton quantum number M_p.

The tensor $\mathfrak{T}^\alpha$ is, as discussed above, axially symmetric about the axis from the proton to the αth fluorine. If this axis is in the z' direction, we are free to choose the x' and y' axes in any way. For any choice of x' and y' axes, $\mathfrak{T}^\alpha$ may be taken to be of the form

$$\mathfrak{T}^\alpha(\mathbf{r}')=\begin{bmatrix}T_\perp & 0 & 0\\ 0 & T_\perp & 0\\ 0 & 0 & T_\parallel\end{bmatrix}, \quad (4)$$

where $\mathbf{r}'$ labels the fact that $\mathfrak{T}^\alpha$ is expressed in its principal axis system. It is necessary to express $\mathfrak{T}^\alpha$ in the laboratory coordinate system in which the z axis is parallel to H_0. Let $\mathbf{r}=(x,y,z)$ represent a vector in this system. If we choose x' and y' such that x', z', x, and z lie in the same plane, then a vector $\mathbf{r}'$ in the principal axis system may be related to r in the laboratory system by a rotation about the $y=y'$ axis by the rotation operator $R(\theta)$: $\mathbf{r}=R(\theta)\mathbf{r}'$, where θ is the angle between $\mathbf{r}$ and $\mathbf{r}'$. Then in laboratory coordinates we have:

$$\mathfrak{T}^\alpha(\mathbf{r})=R(\theta^\alpha)\mathfrak{T}^\alpha(\mathbf{r}')R(\theta^\alpha)^{-1},$$

where

$$R(\theta^\alpha)=\begin{bmatrix}\cos\theta^\alpha & 0 & \sin\theta^\alpha\\ 0 & 1 & 0\\ -\sin\theta^\alpha & 0 & \cos\theta^\alpha\end{bmatrix}.$$

Hence

$$\mathfrak{T}^\alpha(\mathbf{r})=\begin{bmatrix}T_\perp+(T_\parallel-T_\perp)\sin^2\theta^\alpha & 0 & (T_\parallel-T_\perp)\sin\theta^\alpha\cos\theta^\alpha\\ 0 & T_\perp & 0\\ (T_\parallel-T_\perp)\sin\theta^\alpha\cos\theta^\alpha & 0 & T_\perp+(T_\parallel-T_\perp)\cos^2\theta^\alpha\end{bmatrix}. \quad (5)$$

We may write the αth fluorine hyperfine interaction in terms of a local field produced at the fluorine nucleus by the electron: $[\mathbf{S}\cdot\mathfrak{T}^\alpha]\cdot\mathbf{I}^\alpha \equiv -g_F\beta_N\mathbf{H}_L\cdot\mathbf{I}^\alpha$. Because of the large field H_0, the expectation value of $\mathbf{S}$ is parallel to H_0: We obtain the semiclassical approximation which contains still all the principal physical effects by taking $\mathbf{S}=M_s\hat{z}$. The neglected terms lead to small corrections which are treated in detail in Sec. III. We obtain

$$-g_F\beta_N H_L=(0,0,M_s)\cdot\mathfrak{T}(\mathbf{r})$$
$$=M_s((T_{II}-T_\perp)\sin\theta\cos\theta,0,T_\perp+(T_{II}-T_\perp)\cos^2\theta). \quad (6)$$

We have left off for simplicity the superscript α. The local field seen at the αth fluorine nucleus thus consists of a field H_{II} parallel to H_0 and a field $H_\perp$ perpendicular to H_0, where

$$g_F\beta_N H_{II}=T_\perp+(T_{II}-T_\perp)\cos^2\theta,$$

and

$$g_F\beta_N H_\perp=(T_{II}-T_\perp)\sin\theta\cos\theta.$$

The magnitude of $\mathbf{H}_L(M_s)$ is given by $|H_L(M_s)| = |-M_s|\,|(H_\perp,0,H_{II})|$:

$$|H_L(M_s)|=\tfrac{1}{2}[H_\perp^2+H_{II}^2]^{1/2}$$
$$=(1/2g_F\beta_N)[T_\perp^2+(T_{II}^2-T_\perp^2)\cos^2\theta]^{1/2} \quad (7)$$

and the angle between the local field $\mathbf{H}_L$ and $\mathbf{H}_0$ is given by

$$\phi=\tan^{-1}(H_\perp/H_{II})=\tan^{-1}\left[\frac{(T_{II}-T_\perp)\sin\theta\cos\theta}{T_\perp+(T_{II}-T_\perp)\cos^2\theta}\right]. \quad (8)$$

The total field experienced by the αth fluorine is thus

$\mathbf{H}_{\text{total}}=(-H_\perp M_s,0,H_0-H_\perp M_s)$, so

$$|\mathbf{H}_{\text{total}}(M_s)|=[\tfrac{1}{4}H_\perp^2+(H_0-H_{II}M_s)^2]^{1/2}. \quad (9)$$

$\mathbf{H}_{\text{total}}$ makes an angle ψ with respect to $\mathbf{H}_0$ given by

$$\psi=\tan^{-1}[-H_\perp M_s/(H_0-H_{II}M_s)]. \quad (10)$$

These relations are illustrated in Fig. 5.

Because the local field is about 12 kG while H_0 is about 3 kG, the direction of the total field for $M_s=+1/2$ is nearly, *but not exactly*, 180° away from the direction for $M_s=-1/2$. The magnitudes in the two cases are roughly equal. In each case we should properly quantize the fluorine nuclear spin operators along $\mathbf{H}_{\text{total}}(M_s)$. Since in our problem ψ differs from 0° or 180° by less than 45° we may label without ambiguity the nuclear states such that $|+\rangle$ means $\langle I_z\rangle$ has a positive projection along H_0 and $|-\rangle$ means $\langle I_z\rangle$ has a negative projection along H_0. With this convention for labeling the fluorine states, we write the interaction energies of the four states $|M_s\rangle|M_F{}^\alpha\rangle$ for the αth fluorine nucleus:

$$E^\alpha(M_s,M_F{}^\alpha)$$
$$=2M_sM_F{}^\alpha g_F\beta_N[H_\perp^2M_s^2+(H_0-H_{II}M_s)^2]^{1/2}. \quad (11)$$

The total fluorine hyperfine energy is

$$E_{\text{hfs}}=\sum_{\alpha=1}^{8}E^\alpha(M_s,M_F{}^\alpha).$$

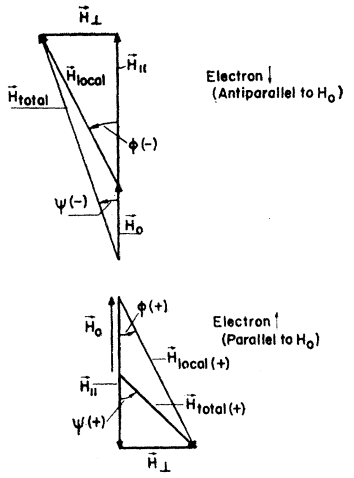

FIG. 5. Geometry of internal and external magnetic fields at a fluorine nucleus, illustrating the approximate conditions responsible for the "forbidden" transitions visible in Figs. 2 and 3.

The fact that the spacing between the fluorine M_F levels depends on the z projection of the electron mirrors the intuitive impression that the local and external fields can be either mainly in opposition to each other, or can mainly aid each other to produce a total field of slightly differing magnitude in the two cases. The fact that the direction of the total field is different for the two electronic states has no effect on the energies. These arguments justify our qualitative description of the superhyperfine interactions in the beginning of this section.

Following the procedure of Castner and Känzig[12] we find it useful, here and in the next section, to quantize the fluorine spin along the local rather than the total field. This expedient has the advantage of giving the hyperfine energies to within a few percent for arbitrary orientation, and of giving the exact expression (11) for $\theta=0°$ and 90°, for which data are available from the (100) and [11$\bar{2}$] spectra. The hyperfine energy for the αth fluorine spin is approximately

$$E^\alpha(M_s,M_F{}^\alpha)=M_F{}^\alpha\{M_s[T_\perp^2+(T_{II}^2-T_\perp^2)\cos^2\theta^\alpha]^{1/2}$$
$$-g_F\beta_N\cos\phi\}. \quad (12)$$

The observed quantities in the resonance experiment are the energy differences between the initial and final states of the system. The contributions to this energy difference due to the hyperfine interaction of the electron and the αth fluorine are, from (12),

$$\Delta E_{\text{hfs}}(M_F{}^\alpha)=M_F{}^\alpha[T_\perp^2+(T_{II}^2-T_\perp^2)\cos^2\theta^\alpha]^{1/2}. \quad (13)$$

Thus, apart from g-value corrections, the slight mixing of electronic states by the electron-proton interaction, and second order corrections in the fluorine system—all of which we will show in Sec. III to be small effects—the interval in magnetic field corresponding to the energy difference between $M_F{}^\alpha=+1/2$ and $M_F{}^\alpha=-1/2$

[12] T. G. Castner and W. Känzig; J. Chem. Phys. Solids 3, 178 (1957).

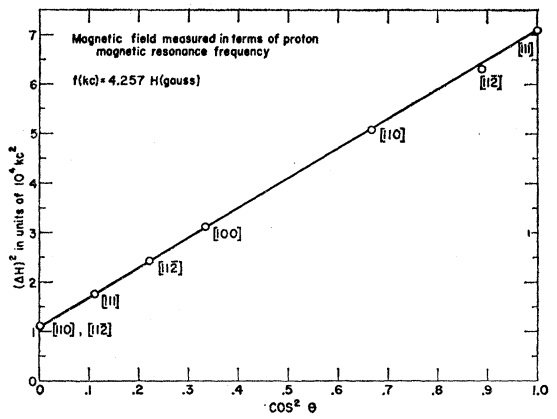

FIG. 6. Plot of the square of the observed magnetic field interval between adjacent ESR lines vs the square of the cosine of the angle between H_0 and the H-F$^-$ axis. The ordinate is expressed in terms of the proton magnetic resonance frequency, $f=4.257$ kc/gauss. The point labeled $[11\bar{2}]$ at $\cos^2\theta\cong 0.9$ is believed to be in error and was not used to find T_{II} and $T_\perp$.

is seen to be simply

$$\Delta^\alpha(H)=(1/g\beta)[T_\perp^2+(T_{II}^2-T_\perp^2)\cos^2\theta^\alpha]^{1/2}. \quad (14)$$

The experimental data, fitted to the square of this equation, are presented in Fig. 6. Values of $T_\perp$ and T_{II}, subject to the corrections mentioned above, are obtained directly from the intercepts at $\cos^2\theta=0$ and 1, respectively. (See Sec. III).

A cursory examination of Figs. 2 and 3 reveals there is a prominent doublet between each pair of lines whose positions have been derived above. These transitions are "forbidden" transitions similar in nature to those described by Trammel *et al.*[13] and identical to those observed by Clogston *et al.*[2] Although the detailed explanation of these lines has been given by these authors, we will repeat it here since it will turn out that their positions allow us to deduce the relative signs of T_{II} and $T_\perp$.[14]

The "forbidden" transitions correspond to the selection rule $\Delta M_s=\pm 1$, $\Delta M_F=\pm 1$. They occur because $\mathbf{H}_{\text{total}}$ is reoriented neither by exactly 0° nor by exactly 180° when an electronic transition occurs. The initial fluorine state $|M_F\rangle$, quantized along the total field $\mathbf{H}_{\text{total}}$ $(M_s=+1/2)$, will under these circumstances have a nonzero projection upon the final fluorine states $|M_F\pm 1\rangle$, quantized along $\mathbf{H}_{\text{total}}$ $(M_s=-1/2)$. Thus, each line of the simple spectrum, corresponding to $\Delta M_F=0$, will give rise to a doublet (with the exception of the end lines of the spectrum for which only either $\Delta M_F=+1$ or $\Delta M_F=-1$ is allowed). These forbidden transitions correspond to a change in hyperfine energy given typically by

$$\Delta E=E(++)-E(-,-)=g_F\beta_N H_0\cos\phi. \quad (15)$$

The field interval $\delta(H)$ between a "forbidden" line and the adjacent allowed line is

$$\delta(H)=\tfrac{1}{2}\Delta(H)-(g_F\beta_N/g\beta)H_0\cos\phi. \quad (16)$$

The intensity of a forbidden line depends on the strength of the perpendicular component of the local field at the fluorine nucleus. Clogston *et al.*[2] give the following expression for the ratio of the transition probability for forbidden transitions relative to allowed transitions:

$$\tan^2\{\tfrac{1}{2}[\psi(M_s=+1/2)-\psi(M_s=-1/2)]\}. \quad (17)$$

Investigation of this relation shows that for our case the relative forbidden to allowed strength should increase with H_0. This effect is already evident in Figs. 1 and 3 if one compares the low- and high-field groups. Comparison of the X- and K-band data shows an increase in the relative strengths of the forbidden transitions by a factor of (5.7 ± 0.5). Equation (17) predicts an increase under these circumstances of a factor of 5.7.

Equation (14) shows that one can only obtain $|T_{II}|$ and $|T_\perp|$ by measuring $\Delta(H)$. Equation (16) shows that the field between an allowed line and an adjacent forbidden line depends on $\cos\phi=(T_{II}-T_\perp)(g\beta\Delta)^{-1}\times\sin\theta\cos\theta$. The observed allowed forbidden field interval is given by (14) to within 10% by the assumption that $T_\perp/T_{II}\leqslant 0$, and to within 0.01% by the assumption that T_{II} and $T_\perp$ are of the same sign.

We should mention that at high microwave powers it is possible to observe on each side of an "allowed" transition, partially resolved satellite lines which are separated in field from the allowed line by one fluorine Zeeman interaction. These transitions arise, most probably, from simultaneous electron and nuclear spin flips involving the 24 next-nearest-neighbor fluorine nuclei. The magnetic interactions of these nuclei with the electron are described in detail in Sec. IV. There it is shown that these electron-fluorine interactions are much smaller than the nuclear Zeeman interaction. These satellites, then, are of the same type as observed by Trammel *et al.*[13] They correspond to the case that the total field at the fluorine changes direction by an angle close to 0° when an electron spin flips. Some indication of these satellites may be seen in Figs. 2 and 4.

III. ACCURATE DETERMINATION OF B, g, AND $\mathfrak{T}^\alpha$

As remarked in the introduction, interest in the g factor in Eq. (1) lies in its small deviation from the free hydrogen value. In this section we obtain the appropriate eigenvalues of (1) to the required accuracy, and then develop expressions from which we may extract the experimental values of B and g of Eq. (1) from the experimental data. It will develop that our knowledge of T_{II} and $T_\perp$ from the approximate treatment of Sec. II is sufficient for our present needs.

[13] G. T. Trammell, Henry Zeldes, and Ralph Livingston, Phys. Rev. **110**, 630 (1958).

[14] See also Baker, Hayes, and O'Brien, Proc. Roy. Soc. (London) **A254**, 272 (1960).

We are concerned here solely with the positions of the $M_F=0$ lines: those for which, roughly speaking, the total projection of the fluorine spin along H_0 is zero. We may measure the positions of these two lines to $\pm 1:10^5$; we are thus required to find the eigenvalues of (1) to this accuracy. Such an accuracy places, in fact, a severe requirement on our ability to align a single crystal in the microwave cavity. Our ability to measure the position of a resonance for a given orientation greatly exceeds our ability to know and reproduce the orientation. For this reason we have measured the spectrum of a powdered sample. The only contributions to the pair of lines (one for each proton orientation) are from the $M_F=0$ components of the singlet and triplet states of the pairs of fluorine nuclei along the body diagonal of the fundamental cube. Except for a few crystallites ($\sim 1\%$ of the total) the only degeneracy among the fluorine nuclear spins is the fundamental pair-wise degeneracy imposed by symmetry. The theoretical problem is also greatly simplified by this experimental expedient, since there is now no necessity of treating, for example, the case of 70-fold degeneracy, which would occur for H_0 parallel to the [100] direction.

In Sec. II we have obtained the eigenvalues of (1) in the approximation that we have ignored terms in (1) connecting different electron spin states. In this approximation the transitions corresponding to $\Delta M_s=\pm 1$, $\Delta M_p=0$, $\Delta M_F=0$ between $M_F=0$ states of the fluorine system appear at fields unmodified by the fluorine hyperfine energy. The neglected matrix elements are on the order of 100 Mc/sec, the fluorine hyperfine energy, so the energy shift which we will compute here will be on the order of $(100)^2/g\beta H=(100\text{ Mc/sec})^2/10^4\text{ Mc/sec}=1$ Mc/sec. One sees that the correction we aim to calculate will be a substantial fraction of the total linewidth of about 5 Mc/sec.

The full hyperfine interaction is

$$\mathbf{S}\cdot\mathfrak{T}\cdot\mathbf{I}=(S_z b\sin\theta\cos\theta,0,S_z(\mathrm{T}_\perp+b\cos^2\theta))\cdot(I_x,I_y,I_z)$$
$$+(S_x(\mathrm{T}_\perp+b\sin^2\theta),S_y\mathrm{T}_\perp,Sb\sin\theta\cos\theta)\cdot(I_x,I_y,I_z), \quad (18)$$

where $b=\mathrm{T}_{\parallel}-\mathrm{T}_\perp$. Here the (x,y,z) coordinate system is the laboratory system, with $\hat{H}_0\equiv\hat{z}$. In the calculation that follows we will find it convenient to quantize $\mathbf{I}$ along $\mathbf{H}_{\text{local}}$, rather than $\mathbf{H}_{\text{total}}$. The fractional error in the correction to the hyperfine energy we are calculating here is $H_0^2\sin^2\phi/H_L^2\leqslant 0.1$. 10% of the expected 1-Mc/sec correction is 100 kc/sec or 150 cps in the frequency of the proton field marker, which is on the order of the scatter in the reproducibility of the data.

We wish to express the operators $(\mathbf{S}\cdot\mathfrak{T})$ and $\mathbf{I}$ in the coordinate system defined by $\mathbf{H}_{\text{local}}=\hat{z}''$. This corresponds to a rotation in the x-z plane through the angle $(+\phi)$, defined by Eq. (8). In Sec. II we have already calculated the major contribution to the hyperfine energy, which comes from those terms in $(\mathbf{S}\cdot\mathfrak{T})_{z''}$ which involve the operator S_z. The perturbation we are interested in here may therefore be written:

$$H_1=\mathbf{I}''\cdot[(\mathbf{S}\cdot\mathfrak{T})''-\hat{z}''\Delta(\theta)]$$
$$=[S_xI_{x''}\mathrm{T}_{\parallel}\mathrm{T}_\perp/\Delta(\theta)]+S_yI_{y''}\mathrm{T}_\perp$$
$$+S_xI_{z''}b\sin\theta\cos\theta(\mathrm{T}_{\parallel}+\mathrm{T}_\perp)/\Delta(\theta). \quad (19)$$

For notational simplicity we drop the double primes on I, remembering that I_z is now diagonal. It is convenient to rewrite H_1 using the raising and lowering operators I^+, I^-, S^+, S^-.

$$H_1=S^+[A_1I^+ +A_2I_z+A_3I^-]$$
$$+S^-[A_3I^+ +A_2I_z+A_1I^-], \quad (20)$$

where

$$A_1=\tfrac{1}{4}\mathrm{T}_\perp[(\mathrm{T}_{\parallel}/\Delta)-1],\quad A_2=b\sin\theta\cos\theta(\mathrm{T}_{\parallel}+\mathrm{T}_\perp)/2\Delta,$$
$$A_3=\tfrac{1}{4}\mathrm{T}_\perp[(\mathrm{T}_{\parallel}/\Delta)+1]. \quad (21)$$

All of these considerations apply for each of the 8 fluorine nuclei, so the total perturbation is the sum of 8 terms of the type (20).

This sum may be separated into 4 terms, each of which pertains to the pair of nuclei which lie along the same body diagonal. Since in the absence of H_1 each pair has exactly degenerate energy levels, it is convenient to work in the total angular momentum representation for each pair. For the moment we confine our attention to a single nuclear pair. We define $\mathbf{I}=\mathbf{I}_1+\mathbf{I}_2$ for each pair separately. The appropriate perturbation for the pair is, accordingly

$$H_p=S^+[A_1I^+ +A_2I_z+A_3I^-]$$
$$+S^-[A_3I^+ +A_2I_z+A_1I^-]. \quad (22)$$

H_p does not connect levels of different I^2 in the $|I,M_I\rangle$ representation. Consequently we may use ordinary nondegenerate perturbation theory. It is at this point that the calculation for H_0 parallel to [1,0,0] becomes awkward because of the seventy-fold degeneracy of the $M_I=0$ state. We defer discussion of the [1,0,0] orientation to Appendix A.

Since the perturation affects only one nuclear pair at a time, and the proton not at all, the appropriate energy corrections are calculated for each pair separately. We need only $\Delta E(M_s,I,M_I)$ for $M_s=\pm\frac{1}{2}$, $I=1$, $M_I=0$, and $I=0$, $M_I=0$. Standard second-order perturbation theory gives

$$\Delta E(M_s,1,0)=4(A_1^2+A_3^2)M_s/h\nu,$$

and

$$\Delta E(M_s,0,0)=0.$$

The energy shift in the $M_s=\pm 1$ microwave transition for the $I=1$, $M=0$ state is thus $4(A_1^2+A_3^2)/h\nu$. When we include all four pairs, we see that each hydrogen atom resonance transition consists of five lines whose type, statistical weight, and frequency shifts are tabulated in Table I. The five components are seen from Table I to be symmetrically disposed about an average energy shift of $8(A_1^2+A_3^2)/h\nu$ from the position expected on the basis of the calculation of Sec. II (which is diagonal in M_s).

TABLE I. Second order hfs of a pair of fluorine nuclei.

Statistical wt.	Type of state	Shift[a]
1	4 singlet	0
4	3 singlet, 1 triplet $M=0$	1
6	2 singlet, 2 triplet $M=0$	2
4	1 singlet, 3 triplet $M=0$	3
1	4 triplet, $M=0$	4

[a] Shift in units of $4(A_1^2+A_3^2)/h\nu$.

Before passing on to calculate the position of the center of the resonance transition for the powder it is worth remarking that the splitting of the singlet and triplet $M=0$ levels calculated in this section is the same as that found by Castner and Känzig[12] for the V_k center. Of course, their Hamiltonian is formally the same as ours. The difference of energies of the singlet and triplet $M=0$ states is just the manifestation of an electron-coupled nuclear pseudo-dipolar interaction, the magnitude of which, about 1 Mc/sec, is a hundred times greater than the direct dipole interaction between the fluorine nuclei.

The calculation of the line shape in the powder expected on the basis of the above calculation is by no means easy. Each crystallite of the powder gives a set of five lines of relative intensity 1:4:6:4:1, each split from its neighbors by $T_\perp^2(T_{11}^2/\Delta+1)/h\nu=4(A_1^2+A_3^2)/h\nu$. The powder line contains contributions from each crystallite, with relatively more crystallites having θ near 90° giving contributions since the orientations are weighted by $d(\cos\theta)$, the relative probability of orientation. Unfortunately the angular dependence of the splitting is not a simple function of $\cos\theta$, so we have not been able to obtain an analytic expression for the powder line shape. It is an experimental fact, one which is examined in detail in the next section, that the width of each resonance line whose position we have calculated here is about 5.3 Mc/sec, whereas the largest splitting between components calculated here is about 7.0 Mc/sec, for $\theta=90°$. Thus, the asymmetric shape which would be predicted on the basis of an exact calculation might well not be detectable experimentally. There is, of course, a shift in the center of the resonance. We have estimated that shift by plotting the line shape expected from 113 randomly oriented crystallites. The shape is, as expected, rather strangely asymmetric, but we see no reason why the peak of the absorption should not occur very close to the center of gravity of the pattern, which is at $7T_\perp^2/h^2\nu_0\equiv E_2/h$ in frequency units away from the unshifted position.

We are now in a position to total the several contributions to the energy of an initial state and to its corresponding final state and write the energy conservation equation for the microwave transition which connects them.

$$h\nu=E_f(\text{H atom})-E_i(\text{H atom})+E_f(\text{first-order hfs})-E_f(\text{first-order hfs})+E_f(\text{second-order hfs})-E_i(\text{second-order hfs}). \quad (23)$$

The energies for the hydrogen atom, E_f(H atom) and E_i(H atom), are obtained exactly from the Breit-Rabi formula. The first order hfs energies are zero for the particular transitions we are considering (in the powder), and we have just calculated the second-order hfs. We obtain the numerical results by three distinct steps: (1) Approximate values of T_{11} and $T_\perp$ are obtained from the study of the superhyperfine spectra of a single crystal (see Sec. II); (2) the second-order hfs energy is obtained using these approximate values of T_{11} and $T_\perp$. From Eq. (2) we obtain g and the proton hyperfine coupling constant B. (3) Using g and B we then obtain better values of T_{11} and $T_\perp$. Further small corrections arising from the second-order terms, as well as from the admixture of hydrogen atom states are also necessary. Further iteration to find better values of g and B is not required.

Values of T_{11} and $T_\perp$ were obtained from the Δ^2 vs $\cos^2\theta$ plot of Sec. II. The results are obtained in magnetic field units. Conversion to frequency units is first made using the free H-atom g value, g_0. The observed microwave transitions are at magnetic fields which satisfy the equations:

$$\begin{aligned} h\nu&=W(1,1)-W(0,0)+E_2 \quad \text{(low-field line)},\\ h\nu&=W(1,0)-W(1,-1)+E_2 \quad \text{(high-field line)}. \end{aligned} \quad (24)$$

The known experimental data are the microwave frequency and the fields-for-resonance. The g value may be extracted from (24) with B eliminated, yielding

$$(g/g_0)^2[w^2(1+y/s)]-(g/g_0)\{2y[3/2+2y/s+\tfrac{1}{2}(w/s)^2]\}+[2+3y/s+1w/s)^2]=0, \quad (25)$$

where $w^2=f_uf_l/v^2$, $y=(f_u+f_l)/2v$, $s=g_0\beta/g_P\beta_N=658.216$, and $v=\nu/s-E_2/sh$.[15] f_u and f_l are the proton resonance frequencies at the fields of the upper and lower field lines, respectively. ν is the microwave frequency scaled by s to express it as the frequency which would give proton resonance in the same magnetic field that a $g=g_0$ sample would give electron spin resonance. One may also solve the pair of Eqs. (24) for B, with the result

$$\frac{B}{s}=\frac{(g/g_0)(f_u-f_l)+(2yg/g_0-1)(f_u-f_l)/s}{2-(g/g_0)y+y/s}. \quad (26)$$

We may now obtain precise values for T_{11} and $T_\perp$. In addition to better values from the accurate value of g, we should also correct Eq. (12) by using the proper hydrogen-atom wave functions:

$$|1\rangle=|-\rangle|+\rangle-\frac{1}{2x}|+\rangle|-\rangle,$$

$$|4\rangle=|+\rangle|+\rangle.$$

[15] The value of $g_J\beta/g_P\beta_N=658.216$ for the hydrogen 1s state is given by E. Lambe, Princeton thesis, 1959 (unpublished). The result is quoted by H. E. Radford, V. W. Hughes, and V. Beltran-Lopez, Phys. Rev. **123**, 153 (1961).

To lowest order in x we now have

$$E_1(M_F)=M_F(1-1/8x^2)[T_\perp^2+(T_{11}^2-T_\perp^2)\cos^2\theta]^{1/2} + (M_F/4x^2)g_F\beta_N H_0. \quad (27)$$

The subscript 1 indicates the fluorine hyperfine interaction has been included only to first order. The corresponding equation for the high-field line has the same form; but note x is field dependent. The second-order fluorine hyperfine energy $E_2(\theta)$ is calculated in Appendix A. When both energies are included, we have

$$\Delta_{obs}(\theta)=E_1(\theta)+E_2(\theta)$$

and hence

$$[T_\perp^2+(T_{11}^2-T_\perp^2)\cos^2\theta]^{1/2} = (1+1/8x^2)\{\Delta_{obs}(\theta)-(g_F\beta_N H_0/4x^2)-E_2(\theta)\}. \quad (28)$$

This equation may be solved for $T_\perp$ at $\theta=90°$, and T_{11} at $\theta=0°$. The final values of T_{11} and $T_\perp$, exhibited in Table II, were obtained from this equation.

Deuterium

The spin Hamiltonian appropriate to the deuterium center is

$$\mathcal{H}=g\beta H_0 S_z+C\mathbf{I}_d\cdot\mathbf{S}-g_d\beta_N H_0 I_{dz} + \sum_{\alpha=1}^{8} S\cdot\mathfrak{T}_d^\alpha\cdot\mathbf{I}^\alpha-g_F\beta_N H_0\sum_{\alpha=1}^{8} I_z^\alpha. \quad (29)$$

The hyperfine coupling constant C is smaller for deuterium than for hydrogen by a factor of 7. For this reason it is tempting to abandon the apparatus developed to treat the hydrogen problem, and extract answers based on simpler approximations. However, it should be appreciated that the interest in the deuterium problem lies in small differences in g, T_{11}, and $T_\perp$ from the hydrogen values, and in the deviation of B/C from the free atom value. For this reason we choose to determine the parameters of the deuterium Hamiltonian by a procedure exactly analogous to that used for hydrogen.

The deuterium spectrum simply repeats the superhyperfine structure three times, corresponding to spin orientations of the deuteron of $M_d=\pm1, 0$. The superhyperfine transitions corresponding to the $M_d=0$ configuration depend on C only in second order. The central line of that group depends on the fluorine hyperfine interaction also only in second order. Hence, we may expect to obtain rather accurate values of T_{11} and $T_\perp$ from the central group, and quite accurate values of g and C from the experimental data substituted into expressions analogous to (25) derived from the Breit-Rabi formula for deuterium. These expressions are obtained in a straightforward manner, but suffer from algebraic complexity, so they will not be reproduced here.

It can be seen from Table II that, in fact, the values of the deuterium spin Hamiltonian parameters are not quoted with as much precision as are the ones for hydrogen. The poorer precision is a consequence of several experimental factors. The primary hyperfine splitting in the deuterium case is comparable to the superfine interaction. Hence, resonance lines in the single-crystal data are occasionally difficult to identify and their centers hard to locate because of "interference" between two or more lines. However the parameters g and C were made on a powdered sample to which both D_2-doped and H_2-doped samples contributed. Thus, the parameters C and g for the deuterium were determined to the same relative accuracy *in this run* as were B and g for the hydrogen. Our relatively smaller experimental uncertainty of g and B for hydrogen is a consequence of more measurements, particularly measurements at 18 kMc/sec.

The only major experimental result not reported in Table II is the change in splitting of the fluorine hfs lines in the [100] orientation upon cooling to 77°K. This result is, for the proton center,

$$\frac{\Delta(77°\text{K})-\Delta(300°\text{K})}{\Delta(300°\text{K})}=+(0.97\pm0.50)\times10^{-3}.$$

We also quote for future reference the following results:

$$\frac{B(\text{interstitial hydrogen})}{B(\text{free hydrogen})}=\frac{1460.2\pm0.1}{1420.406}=1.0280\pm0.0001,$$

$$\frac{C(\text{interstitial deuteron})}{C(\text{free deuterium})}=\frac{224.930\pm0.3}{218.256}=1.0306\pm0.0014.$$

We also might remark, as pertinent to the ratio just quoted for deuterium, that an analysis of the data on the deuterium center allows us to place an upper limit on the deuteron electric quadrupole interaction of $eqQ<0.4$ Mc/sec.

Finally, it should be remarked that all values of g, B, T_{11}, and $T_\perp$ quoted in Table II fit the data at all angles to within 1/10 the resonance linewidth.

IV. ENDOR AND THE ESR LINEWIDTH

The spin Hamiltonian, (1), with which we have been concerned represents the magnetic interactions between the hydrogen atom in its ground state and the eight surrounding fluorine nuclei. The coupling energies are large enough that essentially all of the structure compatible with the various symmetry requirements is actually resolved in the experiments. To understand the resonance linewidths it is necessary to consider the interaction of the unpaired spin with more distant fluorine nuclei. The next shell consists of 24 fluorine nuclei each at $(11)^{1/2}a_0/2$ from the proton. Here a_0 is the lattice constant of the fluorine sublattice. It is convenient to write the relevant interactions, analogous

TABLE II. The experimental results.

Sample	Temperature	Frequency (kMc/sec)	g/g_0	Interstitial[a] hfs constant (Mc/sec)	$T_{\parallel}$ (Mc/sec)	$T_{\perp}$ (Mc/sec)
Proton powder	Room temperature	9	1.000106±0.000010	1460.26 ±0.10	···	···
Proton powder	Room temperature	18	1.000111±0.000010	1460.118±0.22	···	···
Proton single crystal	Room temperature	9	1.00023[b] ±0.00003	···	173.826±0.300	69.025±0.300
Proton single crystal[c]	77°K	9	1.000000±0.000020	1464.19 ±0.2	···	···
Deuteron powder	Room temperature	9	1.00008 ±0.00003	224.927±0.320	···	···
Deuteron single crystal	Room temperature	9	···	···	171.94 ±0.50	67.69 ±0.50

[a] For protons this constant is the symbol B of Eq. (1); for deuterons it is the symbol C of Eq. (29).
[b] g/g_0 as reported here was measured in the [100] orientation and not corrected for second order fluorine hfs. See Appendix A.
[c] The parameters $T_{\parallel}$ and $T_{\perp}$ were not measured at 77°K, only the splitting $\Delta(100)$. Its value is reported in the text. The value of g/g_0 is inferred, and is appropriate for a powder. The measured quantity was Δg of the $M_F=0$ [100] pattern upon cooling to 77°K from room temperature. The result was $\Delta g/g_0=-(98\pm15)\times10^{-6}$.

to (1), in the form

$$\mathcal{H}^E=-g_F\beta_N H_0\sum_{\alpha=1}^{24} I_z^{\alpha}+a\mathbf{S}\cdot\sum_{\alpha=1}^{24}\mathbf{I}_{\alpha}$$
$$+\tfrac{1}{2}b\sum_{\alpha=1}^{24}(3I_z^{\alpha}S_z-\mathbf{I}^{\alpha}\cdot\mathbf{S})(3\cos^2\theta^{\alpha}-1), \quad (30)$$

where θ^{α} is the angle between $\mathbf{H}_0$ and the vector $\mathbf{r}_{\alpha}$ from the proton to the αth fluorine in the second shell. Note that this Hamiltonian is axially symmetric about $\mathbf{r}_{\alpha}$. This approximation is found to give only reasonable account of the angular dependence of the F-center ENDOR lines of LiF and other alkali halides. However we shall see that our data may be fit very well by Eq. (30). Because of the strong electrostatic interaction with the proton in the present case, the unpaired electron is very well localized compared with the F-center electron; thus we may expect the magnetic interaction with distant fluorines to be very much like that between semiclassical point dipoles.[16]

In computing the eigenvalues of (30), we may ignore the nondiagonal operator components, which would lead to electron-coupled pseudodipolar interactions between nuclei of the second shell. These effects are unobservably small because of the smallness of the constants a and b. We obtain the following energy levels for the αth nucleus in the second shell:

$$E_{\alpha}(M_F,M_s)=-g_F\beta_N H_0 M_F$$
$$+M_F M_s[a+b(3\cos^2\theta^{\alpha}-1)]. \quad (31)$$

The ENDOR frequencies are given by

$$h\nu_{\alpha}=h\nu_F\pm\tfrac{1}{2}[a+b(3\cos^2\theta^{\alpha}-1)]. \quad (32)$$

ν_F is the Larmor frequency of fluorine nuclei in the external field H_0.

To compare the expected angular dependence of the ENDOR spectra with experiment and to obtain values for the constants a and b, it is necessary to express the characteristic dipolar angular factor $K(\theta)\equiv(3\cos^2\theta-1)$ of Eq. (32) in terms of the angle which can be changed by rotation of the electromagnet. If [100] is a cube edge, the second shell nuclei are in the directions given by the 24 unit vectors that may be formed by the 24 distinct permutations of the components and signs of the unit vector

$$\mathbf{r}_{\alpha}=\frac{1}{(11)^{1/2}}(\pm3,\pm1,\pm1).$$

In our experiments the CaF_2 crystal was aligned so that a $[1\bar{1}0]$ axis was parallel to the rotation axis of the magnet. Thus H_0 always had equal projections on [100] and [010], and could pass through [001] and [111]. At an arbitrary angle γ from the [001] direction, a unit vector parallel to $\mathbf{H}_0$ has the form

$$\hat{H}_0=(\sin\gamma/\sqrt{2},\sin\gamma/\sqrt{2},\cos\gamma)$$

expressed as $\cos\theta^{\alpha}=\hat{H}_0\cdot\hat{r}_{\alpha}$. Working out the angular factor $3\cos^2\theta^{\alpha}-1$ in terms of the laboratory angle γ gives the following seven angular functions:

$$K_1=(21/11)\cos^2\gamma+(9\sqrt{2}/11)\sin2\gamma-5/11,$$
$$K_2=(21/11)\cos^2\gamma-(9\sqrt{2}/11)\sin2\gamma-5/11,$$
$$K_3=(21/11)\sin^2\gamma+(6\sqrt{2}(11)\sin2\gamma-8/11,$$
$$K_4=(21/11)\sin^2\gamma-(6\sqrt{2}/11)\sin2\gamma-8/11, \quad (33)$$
$$K_5=(3/11)\sin^2\gamma+(3\sqrt{2}/11)\sin2\gamma-8/11,$$
$$K_6=(3/11)\sin^2\gamma-(3\sqrt{2}/11)\sin2\gamma-8/11,$$
$$K_7=(27/11)\cos^2\gamma-1.$$

These functions are plotted as the smooth solid curves in Fig. 7.

The positions of the experimental ENDOR lines can be fitted correctly with the expressions (33) to within about one-third of the 30-kc/sec ENDOR linewidth. In addition to lines described by (33), we observed at simple orientations such as $H_0\|$ [100], [111], and [110] a few extra lines which we attribute to third shell fluorine nuclei. We find we may fit them with an expression of the form (32) using angular factors $K(\gamma)$ apropos third shell nuclei, with b being within a few percent of the classical dipolar coupling for this shell and $b\gg a$.

The ENDOR results are summarized in Table III,

[16] For Eq. 30 to be strictly correct it is necessary that r_{α} be at least a threefold axis. It is not a threefold axis for the fluorine ions in the second shell, but presumably the smallness of a and b preclude our observation of deviations of the data from axial symmetry about r_{α}.

TABLE III. hfs parameters of first three fluorine ion shells.

Shell No.	R^a	a (Mc/sec)	b (Mc/sec)	(classical dipole) b (Mc/sec)
1	$\sqrt{3}$	103.96 ±0.25	34.93 ±0.16	5.6
2	$\sqrt{11}$	0.415±0.015	0.872±0.015	0.804
3	$\sqrt{19}$	0.020±0.025	0.360±0.025	0.354

[a] Distance from proton to jth shell fluorine in units of $\frac{1}{2}a=1.36$ Å.

where we include for comparison the equivalent a and b parameters for the first shell.

The angular dependences in the ENDOR experiment are a consequence of the symmetry of the paramagnetic center. Thus, the success in properly accounting for the angular dependence of the ENDOR data constitutes a very important corroboration of the proposed model for the environment of the hydrogen atom. The fact that none of the ENDOR lines due to nominally equivalent nuclei were split is suggestive that the crystal is locally perfect, at least out to the second fluorine shell.

We may now compute the contribution of the 24 second shell fluorine nuclei to the second moment of the ESR line. The result, following Van Vleck,[17] is

$$\langle\Delta\nu^2\rangle=\tfrac{1}{4}\sum_{\alpha=1}^{24}[a+b(3\cos^2\theta^\alpha-1)]^2. \tag{34}$$

Because of experimental uncertainties in the alignment of the crystal in the magnetic field, it is more meaningful to compare the second moment of the powder sample lines to (34). The appropriate angular average of (34) is easily obtained and extended to include all fluorine nuclei:

$$\langle\Delta\nu^2\rangle_{\text{powder}}=\tfrac{1}{4}\textstyle\sum_j N_j[a_j^2+\frac{4}{5}b_j^2). \tag{35}$$

The running index j labels the shells 2, 3, . . . , and N_j is the number of fluorine in the jth shell.

We have evaluated (35) over fluorine shells $j=2$ and $j=3$ using the values of a_j and b_j in Table III, and over $j=4$, 5, 6, and 7 using the classical dipolar value for b_j. Using the relation for Gaussian lines that $[\Delta\nu]_{\text{max. slope}}=2[\langle\Delta\nu^2\rangle]^{1/2}$, we find $[\Delta\nu]_{\text{max. slope}}=4.94$ Mc/sec.

To compare with experiment it is necessary to include the contribution of the electron-coupled pseudo-dipole interaction between first shell fluorines. In Sec. III we calculated that the effect of this second-order interaction is to shift the center of the powder sample resonance by $7T_\perp^2/\nu_0\cong 3.6$ Mc/sec at 9.3 kMc/sec. For each crystallite, four of the five unresolved lines due to this interaction are shifted, with shifts ranging from 2 units of $T_\perp^2/\nu_0$ to a maximum of about $30T_\perp^2/\nu_0$, depending upon the orientation of the crystallite in the external field. The resultant envelope for the powder has a full width of about $8T_\perp^2/\nu_0$, about 4 Mc/sec at X band. Since the pattern is not symmetrical, and we do not have a tractable analytic expression for the shape, it is not feasible to make quantitative comparisons with great precision. The data are presented in Table IV. There are four lines to compare, two at each microwave frequency. They are identified in Table IV by the resonant field. The last column gives the "excess" width of the experimental line over the value of 4.94 Mc/sec calculated from (35). We ascribe this "excess" width to the second-order interaction, and point out that the large change in the "excess" width between 9 kMc/sec and 18 kMc/sec is in agreement with one's expectations as to the microwave frequency dependence of the second order interaction. However we cannot explain on this basis the smaller width of the high-field lines as compared to the low-field lines at each frequency. The energy denominator in the second-order interaction involves the microwave frequency, not the magnetic field.

[17] J. H. Van Vleck, Phys. Rev. 74, 1168 (1948).

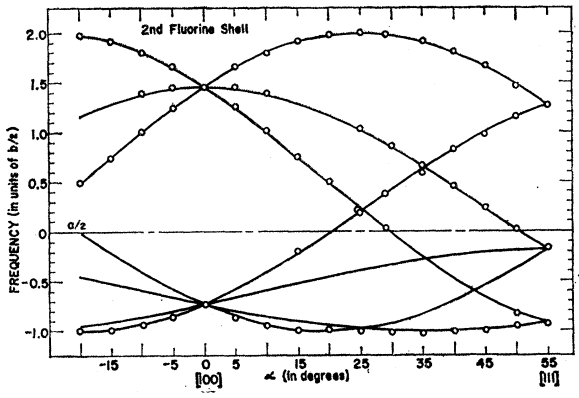

FIG. 7. Angular variation of ENDOR lines for second shell F^- nuclei. Solid lines are graphs of Eqs. (33) in the text. a and b are, respectively, the isotropic and anisotropic hyperfine parameters for the second shell nuclei. The angle α in the figure is the laboratory angle γ in the text. Circles represent experimental points which we were able to assign unambiguously to second shell nuclei.

V. THEORY

The problem of calculating superhyperfine interactions has been of interest to theorists concerned with magnetism since Tinkham's[1] experiments on the fine structure of the paramagnetic resonance spectrum of Mn as a dilute solute in ZnF_2. The spin resonance of the F center in alkali halides led theorists interested in

TABLE IV. Resonance linewidths for powder samples.

Field for resonance (gauss)	Observed width (Mc/sec)	Calculated width[a] (Mc/sec)	"Excess" width (Mc/sec)
3060[b]	(6.26±0.2)	4.94	1.32
3580[b]	(5.98±0.20)	4.94	1.04
6510[c]	(5.63±0.20)	4.94	0.69
7030[c]	(5.37±0.20)	4.94	0.43

[a] Calculated from Eq. (35) in the text. No second-order first shell interactions included.
[b] Microwave frequency ~9 kMc/sec.
[c] Microwave frequency ~18 kMc/sec.

that problem along similar lines.[18] In this section we present a calculation of the hyperfine and superhyperfine parameters based on the simplest approach likely to yield interesting results. A discussion of the various theoretical approaches may be found in the paper by Marshall and Stuart.[3] In their language, the calculation presented here is based on the simple Heitler-London model.

We are required to calculate B, $T_{\parallel}$, $T_{\perp}$, and Δg. It should be noted that only the $\mathfrak{T}$ tensor is calculated in the MnF_2 problem since the Mn hyperfine interaction is not easily susceptible to quantitative calculation. The F-center problem requires Δg and $\mathfrak{T}$ and the hyperfine interactions must be calculated over many shells of neighboring ions. Both the MnF_2 problem and the F-center problem require knowledge of rather complicated wave functions. In our problem we start with one of the simplest possible systems, the hydrogen atom, and expect to calculate, in addition to $\mathfrak{T}$, the magnitude of the wave function at the proton as obtained from B.

We give first a calculation based on the assumption that the interstitial hydrogen atom is fixed at the center of the cube defined by the eight nearest neighbor fluorine ions. Such a calculation is inadequate to account for temperature dependences in B and $\mathfrak{T}^{\alpha}$; nor can it explain the observed difference between the $\mathfrak{T}^{\alpha}$'s for the proton and deuteron.

Under the heading "Dynamic Calculation" we recalculate the hyperfine structure tensors from a simple dynamic model. We will show that the motion of the hydrogen or deuterium atom in its potential well does not alter the magnitudes of these tensors significantly. It does account partially for the small changes in the hyperfine tensor observed after deuteration or cooling to 77°K. These data will be discussed in the light of this dynamic calculation.

A. Static Calculation

We take the electron-nucleus interaction to be of the form

$$\mathcal{H}_{\rm hfs}=2\beta\gamma\hbar\left[\frac{3(\mathbf{I}\cdot\mathbf{r})(\mathbf{S}\cdot\mathbf{r})}{r^5}-\frac{\mathbf{I}\cdot\mathbf{S}}{r^3}+\frac{8\pi}{3}\mathbf{I}\cdot\mathbf{S}\delta(\mathbf{r})\right]. \quad (36)$$

β is the Bohr Magneton, γ is the nuclear magnetogyric ratio of the nucleus of spin $I=1/2$, and $S=1/2$ is the electron spin. For interaction with the proton $\mathbf{r}$ is the electron-proton vector, and for interaction with a fluorine nucleus $\mathbf{r}$ is the electron-fluorine vector. We reduce $\mathcal{H}_{\rm hfs}$ to the spin Hamiltonian (1) by calculating the expectation value of $\mathcal{H}_{\rm hfs}$ with integration over spatial coordinates only. The results of this calculation are, in frequency units,

$$B=(8/3)\gamma_P\beta\langle\psi|\delta(\mathbf{r})|\psi\rangle, \quad (37)$$

[18] For a survey, see B. S. Gourary and F. J. Adrian, in *Solid State Physics*, edited by F. Seitz and D. Turnbull (Academic Press Inc., New York, 1960), Vol. 10, pp. 127–247.

TABLE V. Overlap integrals and their derivatives at $R_{\alpha}=4.46$ au.

	Integral	First derivative	Second derivative
$\langle H\|1s\rangle$	0.0039	−0.0039	0.0032
$\langle H\|2s\rangle$	−0.064	+0.055	−0.038
$\langle H\|2p\sigma\rangle$	0.135	−0.078	0.037
$\langle H\|g_{\alpha}\|2s\rangle$	−0.0056	+0.0054	−0.0059
$\langle H\|g_{\alpha}\|2p\sigma\rangle$	0.025	−0.023	0.023

$$T_{\parallel}{}^{\alpha}=(8/3)\gamma_F\beta\langle\psi|\delta(\mathbf{r}-\mathbf{R}_{\alpha})|\psi\rangle+(1/\pi)\gamma_F\beta\langle\psi|g_{\alpha}|\psi\rangle, \quad (38)$$

$$T_{\perp}{}^{\alpha}=(8/3)\gamma_F\beta\langle\psi|\delta(\mathbf{r}-\mathbf{R}_{\alpha})|\psi\rangle-(1/2\pi)\gamma_F\beta\langle\psi|g_{\alpha}|\psi\rangle. \quad (39)$$

In the above expressions $|\mathbf{R}_{\alpha}|=4.46$ a.u. (atomic units) is the proton-fluorine distance, and $\delta(\mathbf{r}-\mathbf{R}_{\alpha})$ requires that $|\psi|^2$ be evaluated at the fluorine nucleus. $g_{\alpha}=(3\cos^2\theta^{\alpha}-1)r_{\alpha}{}^{-3}$, where r_{α} is the electron-fluorine distance and θ^{α} the angle between r_{α} and R_{α}. In the derivation we have assumed the electron wave function $|\psi\rangle$ to be axially symmetric about each $\mathbf{R}_{\alpha}$.

The argument which allows the use of a one-electron expression for the hyperfine interaction energy is given by Gourary and Adrian.[18] If we assume a purely ionic model for the F^- ions in CaF_2 we require $|\psi\rangle$ to be orthogonal to the core electron wave functions of the eight surrounding fluorine ions. The experimental results strongly suggest that the most reasonable procedure is to start with a simple hydrogen-atom wave function and modify it slightly to achieve the required orthogonality. The appropriate expression for $|\psi\rangle$ is

$$|\psi\rangle=N[|\mathrm{H}\rangle-\sum_{i,\alpha}\langle i_{\alpha}|\mathrm{H}\rangle|i_{\alpha}\rangle], \quad N=[1-\sum_{i,\alpha}|\langle i_{\alpha}|\mathrm{H}\rangle|^2]^{-\frac{1}{2}}. \quad (40)$$

$|\mathrm{H}\rangle=\pi^{-1/2}e^{-r}$ is the free hydrogen atom wave function in atomic units. $|i_{\alpha}\rangle$ is the wave function of the ith orbital on the αth fluorine ion. The summation on α runs over all eight ions, and the summation on i runs over all $1s$, $2s$, and $2p$ orbitals with spin parallel to the H-atom spin.

The values of various integrals required by 37, 38, and 39 are listed in Table V. The appropriate derivatives are also given in anticipation of the discussion of Part B of this section. The fluorine-ion wave functions used were numerical functions of Froese.[19] No attempt was made to follow the suggestion of Marshall and Stuart[3] that free-ion wave functions must be modified for calculations in crystals. We present a brief description of our method of evaluation of the various integrals of Table V in Appendix II.

The results of the calculation are: $B=1660$ Mc/sec, $T_{\parallel}=196$ Mc/sec, and $T_{\perp}=96$ Mc/sec.

These values are all higher by about 10% to 30% than the corresponding experimental values. Considering the simplicity of the calculation the agreement of $T_{\parallel}$ and $T_{\perp}$ with experiment is perhaps surprising.

[19] C. Froese, Proc. Cambridge Phil. Soc. **53**, 206 (1957).

The large value of B, however, must be counted a serious discrepancy, since it is relevant to compare (1660–1420) Mc/sec=240 Mc/sec with (1460–1420) Mc/sec=40 Mc/sec. This discrepancy illuminates the nature of the incompleteness of our calculation. The only crystalline modification of the free hydrogen wave function we have taken into account has been in response to the Pauli exclusion principle, which is effectively a repulsive interaction. The effect of this repulsive interaction is to increase the charge density at the proton over the free atom case, at least for values of R_α as large or larger than $R_\alpha=4.46$ a.u. Other interactions with the crystalline surroundings, such as Van der Waals forces and effects attributable to the dielectric constant of the medium, have the effect of spreading out the wave function and decreasing the charge density at the proton. For hydrogen atoms trapped in rare gas matrices Foner *et al.*[20] have found the attractive interactions can sometimes overcome the repulsive interactions to the extent of decreasing the charge density at the proton from the free atom value.

Adrian,[21] and Jortner and Coulson[22] have estimated the magnitudes of the attractive interactions. We believe estimates of the type they have made are too crude to explain our results. Suppose we begin with a wave function of the type used by Jortner and Coulson: $|H_\lambda\rangle=\lambda^{+3/2}\pi^{-1/2}e^{-\lambda r}$, where $\lambda<1$ is a parameter estimated by a variational technique. Were we to use $|H_\lambda\rangle$ in place of $|H\rangle$ in (40) the desired effect on $\langle\psi|\delta(\mathbf{r})|\psi\rangle$ might be achieved, but inevitably at the expense of larger values of the overlap integrals, since the hydrogenic function clearly spreads farther out into regions where the $1s$, $2s$, and $2p\sigma$ fluorine-ion functions are large. The result would be increased values of T_{11} and $T_\perp$, when these parameters are already too large in the present calculation. What the data seem to require beyond the present calculation is a detailed examination of the effect on the hydrogen atom of the actual crystalline environment. This environment would have to both decrease the overlap integrals somewhat and spread the electron out away from the proton. If we assume the interstitial position is a normally unoccupied body center position, then each hydrogen sees a Ca^{++} ion through the six faces of its cube. If the electron is attracted towards these ions and repelled by electrostatic forces from the fluorines, the desired effect is achieved. In different language, the crystalline potential mixes in $5g$ hydrogenic functions. It is unfortunate the only isotope of Ca with a magnetic moment is 0.13% abundant, since if the above considerations are correct they would lead to a substantial hyperfine interaction with the calcium nucleus, and the data could provide an additional check on more detailed calculations.

A discussion of Δg will be given at the end of the next section. In all the above formulas it was tacitly assumed that $g=2.00$, an assumption sufficiently accurate for the calculations.

B. Dynamic Calculation

The influence of the vibrational state of the hydrogen atom in its potential well on the hyperfine tensors for the U_2 center in KCl has been discussed by Mimura and Uemura.[23] They were, however, unable to compare this aspect of their calculations on the U_2 center to experiment since detailed, precise data such as we have presented here are lacking for the U_2 center.

We start, with Mimura and Uemura, by realizing that if χ is the normalized wavefunction of the hydrogen atom in its potential well in the crystal, we wish to calculate $\langle D_s\rangle=\langle\chi|D_s|\chi\rangle$, where D_s represents $\langle\psi|\delta(\mathbf{r})|\psi\rangle$, $\langle\psi|\delta(\mathbf{r}-\mathbf{R}_\alpha)|\psi\rangle$, or $\langle\psi|g_\alpha|\psi\rangle$. The simplest potential we can envisage which should have some relation to reality is one which allows H-atom motion only in the simple cubic directions in the crystal, i.e., towards any cube face. In three-dimensional language, we have chosen a weak potential along [100] directions, a very strong potential along [111] directions. This choice of potential reduces the problem to that of one-dimensional motion for the H atom and allows us to calculate the value of D_s as a function of the displacement x of the hydrogen atom from its body-center position.

Upon a displacement x of the type described above, the fluorine-proton vector goes from $\mathbf{r}_\alpha=(R_\alpha/\sqrt{3})(1,1,1)$ to $\mathbf{r}_\alpha+\delta\mathbf{r}_\alpha=(R_\alpha/\sqrt{3})(1+x,\ 1,\ 1)$. We assume $x/R_\alpha\ll1$, and keep all terms to x^2. Thus $|\mathbf{r}_\alpha+\delta\mathbf{r}_\alpha|=R_\alpha+\frac{1}{3}x+\frac{1}{6}x^2/R_\alpha$. All of the three integrals D_s may now be calculated at this new position if we assume all electronic wave functions may follow the nucleon motion adiabatically. The results are

$$\begin{aligned}\langle N^2\rangle&=1.21+0.0468\langle x^2\rangle,\\ \langle\langle\psi|\delta(\mathbf{r}_\alpha)|\psi\rangle\rangle&=0.372+0.0129\langle x^2\rangle,\\ \langle\langle\psi|\delta(\mathbf{r}-\mathbf{R}_\alpha)|\psi\rangle\rangle&=0.031+8.6\times10^{-4}\langle x^2\rangle,\\ \langle\langle\psi|g_\alpha|\psi\rangle\rangle&=0.133+2.87\times10^{-3}\langle x^2\rangle.\end{aligned}\tag{41}$$

N is the normalization factor of $|\psi\rangle$. We include it explicitly because the major effect of displacement x on the integrals D_s occurs through the change in normalization. $\langle x^2\rangle=\langle\chi|x^2|\chi\rangle$ is the mean-square vibrational amplitude of the atom in its effectively one-dimensional potential. There is, of course, no term linear in x since $\langle x\rangle=0$. The hyperfine parameters, expressed in frequency units, are

$$\begin{aligned}B&=[1660+57.5\langle x^2\rangle]\text{ Mc/sec},\\ T_{11}&=[196+5.05\langle x^2\rangle]\text{ Mc/sec},\\ T_\perp&=[96+2.9\langle x^2\rangle]\text{ Mc/sec},\\ \Delta(100)&=(\tfrac{1}{3}T_{11}^2+\tfrac{2}{3}T_\perp^2)^{1/2}=[138+3.74\langle x^2\rangle]\text{ Mc/sec}.\end{aligned}\tag{42}$$

[20] S. N. Foner, E. L. Cochran, V. A. Bowers, and C. K. Jen, J. Chem. Phys. **32**, 963 (1960).
[21] F. J. Adrian, J. Chem. Phys. **32**, 970 (1960).
[22] J. Jortner and C. A. Coulson, Molecular Phys. **4**, 451 (1961).
[23] H. Mimura and Y. Uemura, J. Phys. Soc. Japan **14**, 1011 (1959).

$\langle x^2\rangle$ is expressed in units of Bohr radius squared. $\Delta(100)$ is the splitting between superhyperfine structure lines when H_0 is parallel to [100]. We note to begin with that the coefficients of $\langle x^2\rangle$ in each of the above equations are small enough that even $\langle x^2\rangle=1$ amounts to a correction of 2%–3% to the results of the static calculation.

The experimental data we would like to be able to explain are the temperature dependences between 300 and 77°K of B and $\Delta(100)$, and the mass dependences of B, T_{II}, and $T_\perp$. We point out that in both types of data there are apparent anomalies that we are required to explain. A comparison of B with C, the equivalent parameter for the deuteron, shows that there is very little mass dependence of the spin density at the interstitial nucleus. The data on the mixed powdered crystals show an *increase* in the spin density at the deuteron over the proton of $(7\pm5)\times10^{-4}$ a.u. On the other hand, the superhyperfine coupling parameters T_{II} and $T_\perp$ are greater when the interstitial nucleus is a proton than when it is a deuteron by about 1%. Similar anomalies exist in the temperature dependence data. The parameter B increases by 4.2 Mc/sec upon cooling to 77°K from room temperature, whereas $\Delta(100)$ increases by only (0.1 ± 0.05) Mc/sec. Even the fractional increase in B is three times the fractional increase of Δ.

Any attempt to achieve a consistent explanation of these data should allow for the possibility that the fluorine-interstitial nuclear distance may depend on the mass of the interstitial nucleus. If we imagine the static calculation is appropriate to 0°K and to the impossible condition of no vibrational amplitude of the interstitial atom, we may write

$$|\psi_H(0)|^2=|\psi(0)|^2+\left[\frac{\partial}{\partial R}|\psi(0)|^2\right]_{R_\alpha}\delta R_H+0.013\langle x_H^2\rangle,$$
$$|\psi_D(0)|^2=|\psi(0)|^2+\left[\frac{\partial}{\partial R}|\psi(0)|^2\right]_{R_\alpha}\delta R\ +0.013\langle x_D^2\rangle. \quad (43)$$

$|\psi(0)|^2$ and its derivative are the results of the static calculation, δR_H and δR_D represent the change of the fluorine-interstitial nuclear distance due to the presence of the interstitial hydrogen or deuterium, respectively. Subtracting, and multiplying by $(8/3)\beta\gamma_p/a_0^3$ to put in frequency units, we get

$$3.21=407R_{HD}-57.5X_{HD}^2,$$

where the numbers are in Mc/sec, $R_{HD}=[\delta R_H-\delta R_D]$, and $X_{HD}^2=[\langle x_H^2\rangle-\langle x_D^2\rangle]$. The same procedure may be applied to the T_{II} or $T_\perp$ data, either of which yield

$$1.9=-334R_{HD}+5.05X_{HD}^2. \quad (45)$$

Equations (44) and (45) have the solutions $(\delta R_H-\delta R_D)=-0.007$, and $\langle x_H^2\rangle-\langle x_D^2\rangle=-0.1$ in units of a_0 and a_0^2, respectively. These results are at least internally consistent: The larger mean square amplitude for deuterium occurs in a larger box. The same simple harmonic oscillator potential for both H and D always requires $\langle x_H^2\rangle-\langle x_D^2\rangle\geq0$, equality being achieved only in the limit of very high temperatures or weak potential, when the equipartition theorem requires $\langle x^2\rangle=\kappa T/k$ (independent of mass), where k is the simple harmonic oscillator force constant. On the other hand, in a one-dimensional square well potential the quantity $\langle x^2\rangle$ is independent of mass for each individual quantum state, but since the deuteron is twice as massive as the proton the excited state energies are smaller by two than for the proton. Since the value of $\langle x^2\rangle$ is larger the higher the energy of the state, greater thermal excitation of the deuteron implies $\langle x_D^2\rangle-\langle x_H^2\rangle\geq0$, equality obtaining either when both atoms occupy the ground state exclusively or in the very high temperature limit. As an example, with both atoms in the *same* one-dimensional square well of width $2a_0$, and infinite repulsive potential for $|x|\geq a_0$, $\langle x_D^2\rangle-\langle x_H^2\rangle=0.03a_0^2$, and the energy difference between the ground and first excited states is $2\kappa T$ for the proton and κT for the deuteron at room temperature. A quantitative comparison of the mean square amplitudes of vibration and the differences in dilation of the local lattice parameter would require detailed calculations involving the elastic properties of the lattice and will not be attempted here.

We now turn to the temperature dependence data. The same procedure as in the H-D case allows us to write the pair of equations

$$B(77)-B(300)=[\partial|\psi(0)|^2/\partial R]_{R_\alpha}[\delta R_{77}-\delta R_{300}]+0.013[\langle x_{77}^2\rangle-\langle x_{300}^2\rangle], \quad (46)$$
$$\Delta(77)-\Delta(300)=(\partial\Delta/\partial R)_{R_\alpha}[\delta R_{77}-\delta R_{300}]+2.37\times10^{-3}[\langle x_{77}^2\rangle-\langle x_{300}^2\rangle], \quad (47)$$

where $\Delta(T)$ is the splitting between adjacent superhyperfine lines with a H_0 parallel to (100) at the indicated temperature. $\delta R_{77}-\delta R_{300}$ is the difference in R_α at the two temperatures, and $\langle x_{77}^2\rangle-\langle x_{300}^2\rangle$ the difference between the mean square vibrational amplitudes of the hydrogen atom at 77 and 300°K. In megacycle units these equations become

$$4.2=-407R_T+58X_T^2, \quad (48)$$
$$0.12=-255R_T+3.75X_T^2, \quad (49)$$

where R_T and X_T^2 stand for the brackets in Eqs. (46) and (47). The results are

$$\langle x_{77}^2\rangle-\langle x_{300}^2\rangle=0.08a_0^2,$$
$$\delta R_{77}-\delta R_{300}=0.74\times10^{-3}a_0.$$

These results are also internally consistent in the sense that the larger mean square vibrational amplitude goes

with the larger R_α. The remarkable feature of the result is that R_α is larger at 77 than at 300°K, in spite of a thermal contraction of the lattice which alone would require $\delta R_{300}-\delta R_{77}=+0.0137a_0$. It should be noted that there is approximately the same difference between $\langle x_{77}^2\rangle$ and $\langle x_{300}^2\rangle$ as between $\langle x_D^2\rangle$ and $\langle x_H^2\rangle$, whereas the difference between δR_{77} and δR_{300} is an order of magnitude smaller than $\delta R_D-\delta R_H$.

We will not speculate further on these results, but will only acknowledge that the temperature dependence results seem to violate one's physical intuition. We emphasize that the connection between these results and the experimental facts has become very weak, since they depend firstly on a calculation of hyperfine constants, which is accurate only to about 30%, secondly on calculations of derivatives of hyperfine constants which have not been directly compared to experiment, and thirdly on a detailed model of the interstitial nuclear motion which was chosen mainly for simplicity of calculation. On the other hand, as we pointed out before, the experimental facts themselves are not intuitively understandable. A paradox to explain them is not necessarily satisfactory.

We turn finally to the question of the g shift. The most striking feature of this parameter is that it is small but positive when calculated with respect to the free hydrogen atom value. It is interesting to compare Δg with the same quantity for the F center. With the possible exception of the most interesting case for us, LiF, $\Delta g<0$ is observed for all F centers.[18] The experimental results for LiF have been contradictory[24] with the weight of the evidence seeming to be towards a small negative value. A mechanism responsible for a negative Δg has been discussed by Adrian,[25] and calculations by him and by Blumberg and Das[26] yield results in qualitative agreement with experiment for the F center. The essential point of the argument for the F center must apply to our experiment also: The admixture of fluorine ion $2p\sigma$ wave functions in the hydrogen atom electron causes the electron to experience strong spin-orbit forces which are manifested in the spin Hamiltonian by a shift in the g factor. The interesting feature of this mechanism is that it always predicts a *negative* g shift, in our case about one part in 10^4, whereas the measured Δg is *positive* by the same amount. Our experimental accuracy does not allow us to detect a change in Δg between the hydrogen by about $1:10^4$ upon cooling to 77°K. If the g shift were simply related to the vibrational amplitude of the atom in its potential well one might have expected on the basis of the analysis of the previous section that there would by the same change of Δg upon deuteration as upon cooling the hydrogen-doped crystal to 77°K. At present we can offer no explanation for the observed g values. It should be noted, however, that positive g shifts were reported by Foner *et al.*[20] for hydrogen in some of the rare gas matrices.

It is clear that additional experiments would be useful in clarifying some of the complications we have raised. In particular, measurement of *all* hyperfine parameters of the spin Hamiltonian (1), as well as Δg, as a function of hydrostatic pressure both at room temperature and at 77°K on the deuteron center as well as the hydrogen center, would probably furnish enough information to resolve some of the problems we have discussed. It is possible that measurements of the spin-Hamiltonian parameters as a function of uniaxial strain could yield much the same information, particularly since a properly chosen strain will cause an electric field gradient at the deuteron and produce an electric quadrupole interaction with the deuteron. We have not estimated this quantity yet to see if a splitting might be observed. Observations of the changes of the hyperfine coupling parameters as a function of pressure and strain could also provide experimental magnitudes for the matrix elements for spin-lattice relaxation if the mechanism for such relaxation is modulation of the hyperfine tensors by the lattice phonons.

VI. CONCLUSIONS

In this paper we have described the magnetic interactions of a hydrogen atom with its surroundings when it is placed in an interstitial position in a CaF_2 lattice. We have shown that the hydrogen atom remains very much as it is in free space, in agreement with the fact that ~90% of the electronic charge of the atom may be contained in the interstitial space defined by the classical ionic radii of the surrounding fluorine ions. The relatively weak magnetic interactions with the surrounding fluorine nuclei have, however, a profound effect on the paramagnetic resonance spectrum of the center. We have measured the resolved interactions with the eight nearest neighbor fluorine nuclei, determined by ENDOR techniques the interactions with the 24 next-nearest-neighbor fluorines, and seen some indication of the interaction of the hydrogen electron with the third shell. These measurements provide a quantitative measure of the localization of the electron on the proton. Our sample preparation technique has allowed us to deuterate the specimen and observe the small mass dependence of the interactions. We have also observed the small changes in the parameters describing the magnetic interactions after the crystal is cooled to 77°K.

Questions which remain to be examined and which have not been seriously studied in this investigation include the mechanism for production of the hydrogen interstitial atom and the mechanism for its thermal bleaching. Nor have we observed any well-defined optical absorption effects which could be uniquely related

[24] Positive g shifts in LiF have been reported by W. W. Lord, Phys. Rev. **105**, 750 (1957) and J. S. Hyde, *ibid.* **119**, 1483 (1960), and negative ones by W. C. Holton and H. Blum, *ibid.* **125**, 89 (1962).

[25] F. J. Adrian, Phys. Rev. **107**, 488 (1957).

[26] W. E. Blumberg and T. P. Das, Phys. Rev. **110**, 647 (1958).

to the presence of the hydrogen. The question of optical bleaching has not been examined at all.

In Sec. V we presented a calculation of the parameters describing the magnetic interactions of the electron with the proton and surrounding eight nuclei. The calculation is presented in the spirit of an inquiry into the results one does obtain with the standard theoretical techniques which have been used previously in more difficult or less well-defined problems, such as the F center or Mn^{++} in ZnF_2. The agreement of this calculation with experiment was found to be only fair—the calculated parameters were up to 30% too large. The calculation was somewhat optimistically extended to a dynamic model in an attempt to understand the small proton-deuteron and temperature differences. It is hoped these attempts will stimulate work which will treat the whole problem properly and which will be satisfied only by excellent agreement with the experiments. It should also be emphasized that a "standard" calculation is inadequate to explain even qualitatively the observed g shifts.

We conclude by emphasizing our belief that we have studied an impurity center which provides unique opportunities for theorists to calculate from basic principles the measured interactions. We have shown that the wave function of this impurity center is quite close in its main features to that of a free hydrogen atom. At the same time the solid-state effects which have caused deviations from free atom behavior are well defined and susceptible to very accurate measurement, and the substitution of the deuteron for the proton allows an additional check on those aspects of the theory which involve local lattice dynamics.

ACKNOWLEDGMENTS

We gratefully acknowledge many conversations with our colleagues, J. S. Langer and J. M. Radcliffe, on the theoretical aspects of this problem. The aid of Professor S. A. Friedberg and Dr. William E. Vehse on some experimental aspects is greatly appreciated. We are also indebted to Professor C. P. Slichter for a valuable suggestion. Professor R. G. Parr, in the Department of Chemistry, provided invaluable aid on the evaluation of the overlap integrals. R. Hartman programed these integrals for the computer.

APPENDIX A. SECOND ORDER hfs CORRECTION FOR $H_0\|[1,0,0,]$

We have remarked that the number of degenerate energy levels of the 8 first shell fluorine nuclei can be quite large for special orientations of the crystal in the external field. For example, for $H_0\|[100]$, the $\sum_{\alpha=1}^{8} M_F^{\alpha}=0$ state is seventy-fold degenerate. We can calculate with certainty the pseudodipolar effects only for the twofold degenerate problem which arises from the "pairwise" degeneracy characteristic of the model. By taking our data for the $\theta=90°$ interaction from the $H_0\|[11\bar{2}]$ spectra and our data for the $\theta=0°$ interaction from $H_0\|[111]$, we have been able largely to skirt the problem, since these alignments produce only single nuclear pairs at the desired angles. This approach is somewhat limited, however, because of the accidental overlapping of lines which occurs at the [111] orientation. Also it is clearly of interest to make detailed comparisons of the observed and predicted superhyperfine spectra at many orientations, especially those which give the best signal/noise and resolution, i.e., those with a high degree of degeneracy. In this Appendix we will focus mainly on the effects of degeneracy upon the second order calculations for the 8 equivalent fluorines of the [100] alignment, since this result is also useful in comparing the [100] g value with the powder sample result. In the process we discover in what sense the nuclei really are equivalent.

Our approach is to follow Sec. III to the extent of starting with four pairs of nuclei of total spin for each pair $I=1$ and 0; $I_z=I_{1z}+I_{2z}$ is the z component of the total angular momentum operator for each pair, and $|M\rangle$ is the eigenfunction of I_z. The second order contribution to the energy of the state $|M_s\rangle|M\rangle$ for each pair is

$$\Delta E_2(M_s,M)=\sum_{M_s'M'}\frac{\langle M_s|\langle M|H_1|M'\rangle|M_s'\rangle\langle M_s'|\langle M'|H_1|M\rangle|M_s\rangle}{E(M_s,M)-E(M_s',M')}. \tag{A1}$$

The perturbation H_1, is given by Eq. (20) in Sec. III. We ignore the mixture of M_s states of the hydrogen atom and approximate the energy denominator by $h\nu$. Contracting on spin coordinates M_s and on nuclear spin coordinates M' we have

$$\begin{aligned}\Delta E_2(-1/2,M)&=-\frac{1}{h\nu}\langle M|H_+^{\dagger}H_+|M\rangle,\\ \Delta E_2(1/2,M)&=\frac{1}{h\nu}\langle M|H_-^{\dagger}H_-|M\rangle.\end{aligned} \tag{A2}$$

In (A2) the perturbation H_1 has been broken into two parts $H_1=S^+H_+ + S^-H_-$.

(A2) demonstrates in clearer form the fact already mentioned in Sec. III that the spin Hamiltonian (1) contains buried within it a bilinear coupling between fluorine nuclei on the same body diagonal. We can see in addition for $H_0\|[100]$ that H_1 produces a coupling among the pairs. From symmetry the strength of the coupling between the various pairs must be the same; the important point concerns their relative phases.

In terms of the laboratory system defined in II, the positions of the fluorine nuclei are described by the following vectors:

$$\begin{aligned}\mathbf{r}_1&=\pm(\sqrt{2},0,1),\\ \mathbf{r}_2&=\pm(0,\sqrt{2},1),\\ \mathbf{r}_3&=\pm(-\sqrt{2},0,1),\\ \mathbf{r}_4&=\pm(0,-\sqrt{2},1).\end{aligned}\tag{A3}$$

A principal axis vector in the r' system, (0,0,1), is transformed into $\mathbf{r}_1$ and $\mathbf{r}_2$ by a rotation through angle $+\theta$ by the rotation operator $R(\theta)$ about the y and x axes, respectively. A vector (0,0,1) is transformed into $\mathbf{r}_3$ and $\mathbf{r}_4$ by $R(-\theta)$ about the y and x axes, respectively. Similarly the angle ϕ between the local field and H_0 is positive for $\mathbf{r}_1$ and $\mathbf{r}_2$, corresponding to a rotation about the y and x axes, respectively, and is negative for $\mathbf{r}_3$ and $\mathbf{r}_4$, corresponding to rotation, respectively, about the y and x axes in the opposite senses. If we proceed as in Sec. III, we are interested in writing $H_1{}^\dagger H_1$ in the $\hat{z}''$ system, where $\hat{z}''$ is in the direction of the local field. This procedure in Sec. III leads to Eq. (19). We can show that the pairs labeled by 1 and 3 in (A3) will differ in the sign of S_x in H_1. The pairs 2 and 4 in (A3) will be the same as 1 and 3 except S_x and I_x will be interchanged with S_y and I_y, and pairs 2 and 4 will differ in the sign of S_y. We may summarize these results by writing the perturbation in the form

$$\begin{aligned}H_+(n)&=[\eta(n)^2A_1I_n{}^+ +\eta(n)A_2I_{nz}+A_3I_n{}^-],\\ H_-(n)&=[A_3I_n{}^+ +\eta^*(n)A_2I_{nz}+\eta^2(n)I_n{}^-],\end{aligned}\tag{A4}$$

where $\eta(n)=(i)^{n-1}$. (A4) is Eq. (20), Sec. III, for any nuclear pair labeled by $n=1, 2, 3, 4$. We have, as in Sec. III, dropped the primes on coordinates in (A4); $I_z=I_{z''}$ is diagonal.

The operators $H_+{}^\dagger H_+$ and $H_-{}^\dagger H_-$ in (A2) are given by the product of the sum over all pairs:

$$\begin{aligned}H_+{}^\dagger H_+&=\textstyle\sum_{nn'} H_+{}^\dagger(n')H_+(n),\\ H_-{}^\dagger H_-&=\textstyle\sum_{nn'} H_-{}^\dagger(n')H_-(n).\end{aligned}\tag{A5}$$

The operators (A5) contain terms which connect states $|M_s\rangle|M\rangle$ which differ by $M=\pm1, \pm2$, as well as terms which connect states which do not differ in their M quantum numbers. It is clear from the form of (A2) that only the latter contribute to ΔE_2. The effect of the remaining terms in (A5) appears only in higher order than we are considering here.

The summation (A5) may be considered in two parts, $n=n'$ and $n\neq n'$. These terms are

$$\begin{aligned}H_+{}^\dagger H_+(n=n')=\sum_{n=1}^{4}\{&A_1{}^2[I_{nz}I_n{}^2(I_{nz}-1)]\\ &+A_3{}^2[I_{nz}-I_{nz}(I_{nz}+1)]+A_2{}^2(I_{nz})^2\},\end{aligned}\tag{A6}$$

$$\begin{aligned}H_+{}^\dagger H_+(n\neq n')=\sum_{n=1}^{4}[&A_1{}^2\eta(n)^2\eta(n')^2I_n{}^-I_n{}^+\\ &+A_2{}^2\eta^*(n)\eta(n')I_{nz}I_{n'z}+A_3{}^2I_n{}^+I_n{}^-].\end{aligned}\tag{A7}$$

Similar expressions can be written for $H_-{}^\dagger H_-$. Note that in (A6) $\eta(n)$ has always appeared to a high enough power to give $+1$. If the signs of the cross terms $I_n{}^+I_n{}^-$, etc. of (A7) were always positive, it would be possible to diagonalize this term by transforming to the Π^2 and Π_z representation, where $\Pi=\sum_{n=1}{}^4 I_n$, $\Pi_z=\sum_{n=1}{}^4 I_{nz}$. If the cross terms of (A7) did not exist at all, the representation labeled by the nuclear pair quantum numbers I, M would be diagonal. However, as things stand neither representation gives an exact answer. Since the size of the second order shift is on the order of $A_1{}^2/h\nu=1$ Mc/sec, which is a fraction of the resonance linewidth, we will content ourselves with two estimates of (A2). We may either arbitrarily take the cross terms to be positive and work in the Π^2, Π_z representation, or neglect them entirely and work in the I, M representation. We perform the estimates for the $M=0$ line.

In the Π^2, Π_z representation the submatrix corresponding to $M_z=0$ is of dimension 70×70. We expect the artifice of taking all cross terms to be positive will overestimate (A2). Equation (A6) gives the energy directly if we read Π and Π_z for I and I_z, and drop the summation. For the purpose of estimating, we average over the $I=0$, 1, 2, 3, 4 states using the statistical weights of 14, 28, 20, 7, 1, respectively. The result is

$$\Delta E_2=4(A_1{}^2+A_3{}^2)/h\nu.\tag{A8}$$

At $\nu=9$ kMc/sec this term represents correction to the [100] g value given by first order theory of only -96 parts per million (ppm).

We obtain the average shift in the pairs-only representation in the same way as in the powdered-sample problem, except that the average over θ is obviously not required. The contribution of each type of nuclear spin state is multiplied by the statistical weight for that state, summed, and the result normalized by division by the total number of states, 70, for the $M=0$ line of the [100] spectrum. The result is:

$$\Delta E_2=8\frac{A_1{}^2+A_3{}^2}{h\nu}+\frac{24}{7}\frac{A_2{}^2}{h\nu}.\tag{A9}$$

At 9 kMc/sec this represents a correction to the g shift as calculated from first-order theory of -298 ppm. The second-order correction for the powder data, a correction in which we can have confidence, was -220 ppm, approximately midway between the two estimates made here.

APPENDIX B. CALCULATION OF OVERLAP INTEGRALS

We are required to evaluate integrals of the form $\langle \mathrm{H}|P_l(\cos\theta_\alpha)f(r_\alpha)|i_\alpha\rangle$, where $\langle \mathrm{H}|=(\pi)^{-1/2}e^{-r}$, and $\langle i_\alpha|$

is a $1s$, $2s$, or $2p$ fluorine function. The angular parts of $\langle i_\alpha|$ are, of course, just the appropriate spherical harmonics, and the radial functions we used are given in the form of numerical tables by Froese.[19] For the overlap integrals $\langle \mathrm{H}|1s\rangle$, $\langle \mathrm{H}|2s\rangle$, and $\langle \mathrm{H}|2p\sigma\rangle$, $P_l(\cos\theta_\alpha)f(r_\alpha)$ is just a constant. In the integral $\langle \mathrm{H}|g_\alpha|i_\alpha\rangle$, $g_\alpha = 2P_2(\cos\theta_\alpha)r_\alpha^{-3}$. We make use of the expansion of e^{-r} about the fluorine nucleus as given by Barnett and Coulson[27]:

$$e^{-r}=\sum_{l=0}^{\infty} P_l(\cos\theta_\alpha)\frac{(2l+1)}{(r_\alpha R_\alpha)^{\frac{1}{2}}}\zeta_{1,l}(1,r_\alpha; R_\alpha).$$

$P_l(\cos\theta_\alpha)$ is the lth order Legendre polynomial; θ_α is the angular position of the electron as measured from the proton-fluorine internuclear line, r_α is the electron's radial coordinate as measured from the fluorine nucleus. $\zeta_{1,l}(1,r_\alpha; R_\alpha)$ is a certain combination of products of $I_{l\pm1/2}(r_\alpha)$, and $K_{l\pm1/2}(r_\alpha)$ as given by Barnett and Coulson. The I and K functions are half-integral Bessel functions of imaginary argument. With this expansion the angular integrals are easily performed, and the radial integrals are of the form

$$\int_0^\infty r_\alpha^2 R_{n,l}(r_\alpha)f(r_\alpha)\zeta_{1,l}(1,r_\alpha; R_\alpha)dr_\alpha,$$

where the fluorine radial functions $K_{n,l}(r_\alpha)$ satisfy the normalization condition $\int_0^\infty \gamma_\alpha^2 R_{u,l}^2(r_\alpha)dr_\alpha=1$. The radial integrals were evaluated by the CIT Bendix G-20 computer using Simpson's rule. The Bessel functions were generated by the computer using a subroutine developed by members of the group of Professor R. G. Parr in the Department of Chemistry. The values of the required integrals were obtained in steps of $0.20a_0$ for R_α between $3.8a_0$ and $5.2a_0$. Derivatives quoted in Table V were obtained graphically.

[27] M. P. Barnett and C. A. Coulson, Phil. Trans. Roy. Soc. (London) **243**, 224 (1950–1951).